Proceedings IRF2018: 6th International Conference Integrity-Reliability-Failure
Lisbon/Portugal 22-26 July 2018. Editors J.F. Silva Gomes and S.A. Meguid
Publ. INEGI/FEUP (2018); ISBN: 978-989-20-8313-1

PAPER REF: 7187

MODAL DECOMPOSITION PROCEDURES FOR FE-BASED STUCTURAL MODELS WITH NON-PROPORTIONAL DAMPING

Evgueni Stanoev(*)
Endowed Chair of Wind Energy Technology, Faculty of Mechanical Engineering and Marine Technology, University of Rostock, Germany
(*)*Email:* evgueni.stanoev@uni-rostock.de

ABSTRACT

This paper presents two variants of a general method (Cramer, Stanoev 2008), (Stanoev 2013, 2014, 2016, 2017) for modal transformation of the equations of motion for multi-degree-of-freedom-systems (MDOFS) with non-modal symmetric damping matrix. The first variant is described in comparison with a similar method, presented in earlier publications (Chu M. T., Buono N. T. 2008), (Ma Fai F., Morzfeld M., Imam A., 2010). The equations of motion are stated in state-space formulation. The final modal decomposition is performed by a purely real-space transformation matrix, which is derived by a combination of two complex transformations using the complex left and right eigenvectors of the associated special eigenvalue problem. The eigenvector normalization is performed in two different ways. Analytical expressions for all presented variants of the modal transformation basis are developed by the aid of computer algebra software. The proposed modal procedures retain all common advantages of the classic modal decomposition of the equations of motion.

Keywords: structural dynamics, modal decomposition, left and right eigenvectors, complex eigenvalue problem, non-proportional damping.

1 INTRODUCTION

The solution of the classic linear eigenvalue problem, associated to the equations of motion of multi-degree-of-freedom-systems (MDOFS), consists of real eigenvalues (natural frequencies) and real eigenvectors. The inclusion of viscous damping in the equations of MDOFS leads to a quadratic eigenvalue problem with corresponding complex conjugate pairs of eigenvalues and eigenvectors.

Starting point of our considerations are the equations of motion of a damped MDOFS in configuration space

$$\boldsymbol{M}\ddot{\boldsymbol{V}} + \boldsymbol{D}\dot{\boldsymbol{V}} + \boldsymbol{K}\boldsymbol{V} = \mathbf{p}(t)\,, \tag{1.1}$$

where $\boldsymbol{M}, \boldsymbol{D}$ and $\boldsymbol{K}$ are, respectively the (n x n) mass, damping and stiffness matrix, and $\boldsymbol{V}, \dot{\boldsymbol{V}}, \ddot{\boldsymbol{V}}$ are respectively the (n x 1) displacement, the velocity and the acceleration vectors and $\mathbf{p}(t)$ is the (n x 1) excitation vector.

In structural mechanics problems the matrices $\boldsymbol{M}, \boldsymbol{D}$ and $\boldsymbol{K}$ are considered to be real, symmetric and positive definite, excluding the presence of rigid body modes. In the classic modal analysis $\boldsymbol{D} = \boldsymbol{0}$, in this case Eq. (1.1) can be decoupled by use of the real right eigenvectors $\mathbf{X}_j$ of the undamped system:

$$\left(\lambda_j^2\,\mathbf{M} + \mathbf{K}\right)\mathbf{X}_j = \mathbf{0} \tag{1.2}$$

In the case of classically damped system with $\boldsymbol{D} \neq \mathbf{0}$ Eq. (1.1) can also be decoupled by the real eigenvectors of the undamped system. According to (T.K. Caughey, 1965) the necessary and sufficient condition for classical damping is:

$$\boldsymbol{D}\boldsymbol{M}^{-1}\boldsymbol{K} = \boldsymbol{K}\boldsymbol{M}^{-1}\boldsymbol{D} \tag{1.3}$$

The proportional damping assumption

$$\boldsymbol{D} = \alpha\boldsymbol{M} + \beta\boldsymbol{K}\,, \tag{1.4}$$

the so-called *Rayleigh damping*, is a particular case of classic damping - Eq. (1.4) satisfies the condition (1.3).

The associated quadratic eigenvalue problem to Eq. (1.1) is

$$\left(\boldsymbol{M}\lambda_j^2 + \boldsymbol{D}\lambda_j + \boldsymbol{K}\right)\boldsymbol{X}_j = \mathbf{0} \tag{1.5a}$$

where $\lambda_j = \alpha_j + i\omega_{Dj}$; $\bar{\lambda}_j = \alpha_j - i\omega_{Dj}$ (1.5b)

are complex conjugate eigenvalues.

This paper presents two variants of a general method (H. Cramer, 2008), (E. Stanoev, 2013, 2014, 2016, 2017) for real-space modal transformation of the equations of motion of multi-degree-of-freedom-systems (MDOFS) with symmetric damping matrix, representing non-proportional damping. The equations of motion are stated in state-space formulation. The first variant, presented in Section 2, is described in comparison with a similar technique for decoupling of non-classically damped system equations, referred to as *phase synchronization*, presented in earlier publications (Chu M. T., 2008), (Fai F. Ma, 2010), (Fai F. Ma, 2011). This approach has been described in (Fai F. Ma, 2009), (Fai F. Ma, 2010) for free and forced vibrations in configuration space formulation. In (Fai F. Ma, 2011) it has been shown the interpretation of the decoupling transformation by phase synchronization on the basis of state space formulation.

The problem of decoupling the homogenous problem of Eq. (1.5) can also be addressed as a reduction of the quadratic pencil $Q(\lambda) = \boldsymbol{M}\lambda^2 + \boldsymbol{D}\lambda + \boldsymbol{K}$. In (S.D. Garvey, 2002) and (M. T. Chu, 2008) have been proposed the notion of *structure-preserving transformations* in diagonalizing $Q(\lambda)$. In (Fai F. Ma, 2011) it has been shown that transformation of (1.1) by phase synchronization can be interpreted as a diagonalizing structure-preserving transformation in state space if the eigenvalues λ_j, $\bar{\lambda}_j$ are complex and distinct.

In Section 3 of this paper is presented a second variant for real-space decoupling procedure, based on both the right and the left complex eigenvector pairs. In this version the complex conjugated eigenvectors for the MDOFS are normalized with respect to the general stiffness matrix.

In order to introduce to the solutions presented in Section 2 and 3, we will first briefly review in section 1.1 the phase synchronization procedure on the basis of state space formulation according to (Fai F. Ma, 2010), (Fai F. Ma, 2011) - for the case of forced vibrations with n distinct complex conjugated eigenvalues λ_j.

1.1 The phase synchronization procedure in state space

We suppose all eigenvalues λ_j, $\bar{\lambda}_j$ in (1.5b) to be complex conjugated and distinct, i.e. the quadratic eigenvalue problem is non-defective.

First of all, Eq. (1.1) should be written in state space in the *symmetric Lancaster form*, see (P. Lancaster, 1966):

$$\begin{bmatrix} \boldsymbol{D} & \boldsymbol{M} \\ \boldsymbol{M} & \end{bmatrix}\begin{bmatrix} \dot{\boldsymbol{V}} \\ \ddot{\boldsymbol{V}} \end{bmatrix} + \begin{bmatrix} \boldsymbol{K} & \\ & -\boldsymbol{M} \end{bmatrix}\begin{bmatrix} \boldsymbol{V} \\ \dot{\boldsymbol{V}} \end{bmatrix} = \begin{bmatrix} \mathbf{p}(t) \\ \end{bmatrix} \tag{1.6}$$

The associated state space eigenvalue problem takes the form

$$\left(\begin{bmatrix} \boldsymbol{D} & \boldsymbol{M} \\ \boldsymbol{M} & \end{bmatrix}\lambda_j + \begin{bmatrix} \boldsymbol{K} & \\ & -\boldsymbol{M} \end{bmatrix}\right)\begin{bmatrix} \boldsymbol{X}_j \\ \lambda_j \boldsymbol{X}_j \end{bmatrix} = L(\lambda_j)\begin{bmatrix} \boldsymbol{X}_j \\ \lambda_j \boldsymbol{X}_j \end{bmatrix} = \mathbf{0}$$

$$\rightarrow \begin{bmatrix} \boldsymbol{K} & \\ & -\boldsymbol{M} \end{bmatrix}\begin{bmatrix} \boldsymbol{X}_j \\ \lambda_j \boldsymbol{X}_j \end{bmatrix} = -\lambda_j \begin{bmatrix} \boldsymbol{D} & \boldsymbol{M} \\ \boldsymbol{M} & \end{bmatrix}\begin{bmatrix} \boldsymbol{X}_j \\ \lambda_j \boldsymbol{X}_j \end{bmatrix} \tag{1.7a,b}$$

The symmetrically linearized pencil $L(\lambda_j)$ is referred to as the *Lancaster structure*.

A complex modal transformation is defined by

$$\begin{bmatrix} \boldsymbol{V} \\ \dot{\boldsymbol{V}} \end{bmatrix} = \begin{bmatrix} \boldsymbol{X} & \overline{\boldsymbol{X}} \\ \boldsymbol{X}\,\boldsymbol{\Lambda} & \overline{\boldsymbol{X}}\,\overline{\boldsymbol{\Lambda}} \end{bmatrix}\begin{bmatrix} \boldsymbol{a} \\ \boldsymbol{b} \end{bmatrix} \tag{1.8}$$

where

$$\boldsymbol{a} = [a_1 \quad a_2 \quad \cdots \quad a_n]^T, \quad \boldsymbol{b} = [b_1 \quad b_2 \quad \cdots \quad b_n]^T \tag{1.9a}$$

are new complex modal coordinates,

$$\boldsymbol{X} = [\boldsymbol{X}_1 \quad \boldsymbol{X}_2 \quad \cdots \quad \boldsymbol{X}_n], \quad \overline{\boldsymbol{X}} = [\overline{\boldsymbol{X}}_1 \quad \overline{\boldsymbol{X}}_2 \quad \cdots \quad \overline{\boldsymbol{X}}_n] \tag{1.9b}$$

are modal matrices built by the complex $\boldsymbol{X}_j$ resp. the conjugate complex eigenvectors $\overline{\boldsymbol{X}}_j$, and

$$\boldsymbol{\Lambda} = \mathrm{diag}[\lambda_1, \lambda_2, \cdots, \lambda_n], \quad \overline{\boldsymbol{\Lambda}} = \mathrm{diag}[\overline{\lambda}_1, \overline{\lambda}_2, \cdots, \overline{\lambda}_n] \tag{1.10}$$

are the associated spectral matrices. The transformation (1.8) implies that the j-th damped mode of vibration $\boldsymbol{s}_j(t)$ is expressed as a linear combination

$$\boldsymbol{s}_j(t) = \boldsymbol{X}_j \underbrace{\left(c_j e^{\lambda_j t}\right)}_{a_j} + \overline{\boldsymbol{X}}_j \underbrace{\left(\overline{c}_j e^{\overline{\lambda}_j t}\right)}_{b_j} \tag{1.11}$$

The eigenvectors $\mathbf{X}_j$ may be normalized in accordance with

$$2\lambda_j \mathbf{X}_j{}^T \boldsymbol{M} \mathbf{X}_j + \mathbf{X}_j{}^T \boldsymbol{D} \mathbf{X}_j = 2i\omega_{Dj} = \lambda_j - \overline{\lambda}_j \quad \text{resp.}$$

$$2\lambda_j \overline{\mathbf{X}}_j{}^T \boldsymbol{M} \overline{\mathbf{X}}_j + \overline{\mathbf{X}}_j{}^T \boldsymbol{D} \overline{\mathbf{X}}_j = -2i\omega_{Dj} = \overline{\lambda}_j - \lambda_j \tag{1.12a,b}$$

Substitute Eq. (1.8) into (1.6) and pre-multiply by $\begin{bmatrix} \boldsymbol{X} & \overline{\boldsymbol{X}} \\ \boldsymbol{X}\,\boldsymbol{\Lambda} & \overline{\boldsymbol{X}}\,\overline{\boldsymbol{\Lambda}} \end{bmatrix}^T$ to obtain

$$\underbrace{\begin{bmatrix} \boldsymbol{X} & \overline{\boldsymbol{X}} \\ \boldsymbol{X}\,\boldsymbol{\Lambda} & \overline{\boldsymbol{X}}\,\overline{\boldsymbol{\Lambda}} \end{bmatrix}^T \begin{bmatrix} \boldsymbol{D} & \boldsymbol{M} \\ \boldsymbol{M} & \end{bmatrix}\begin{bmatrix} \boldsymbol{X} & \overline{\boldsymbol{X}} \\ \boldsymbol{X}\,\boldsymbol{\Lambda} & \overline{\boldsymbol{X}}\,\overline{\boldsymbol{\Lambda}} \end{bmatrix}}\begin{bmatrix} \dot{\boldsymbol{a}} \\ \dot{\boldsymbol{b}} \end{bmatrix} + \underbrace{\begin{bmatrix} \boldsymbol{X} & \overline{\boldsymbol{X}} \\ \boldsymbol{X}\,\boldsymbol{\Lambda} & \overline{\boldsymbol{X}}\,\overline{\boldsymbol{\Lambda}} \end{bmatrix}^T \begin{bmatrix} \boldsymbol{K} & \\ & -\boldsymbol{M} \end{bmatrix}\begin{bmatrix} \boldsymbol{X} & \overline{\boldsymbol{X}} \\ \boldsymbol{X}\,\boldsymbol{\Lambda} & \overline{\boldsymbol{X}}\,\overline{\boldsymbol{\Lambda}} \end{bmatrix}}\begin{bmatrix} \boldsymbol{a} \\ \boldsymbol{b} \end{bmatrix} = \begin{bmatrix} \boldsymbol{X}^T \mathbf{p}(t) \\ \overline{\boldsymbol{X}}^T \mathbf{p}(t) \end{bmatrix}$$

$$\begin{bmatrix} \boldsymbol{X}^T \boldsymbol{D} \boldsymbol{X} + 2\boldsymbol{\Lambda}(\boldsymbol{X}^T \boldsymbol{M} \boldsymbol{X}) & \\ & \overline{\boldsymbol{X}}^T \boldsymbol{D} \overline{\boldsymbol{X}} + 2\overline{\boldsymbol{\Lambda}}\left(\overline{\boldsymbol{X}}^T \boldsymbol{M} \overline{\boldsymbol{X}}\right) \end{bmatrix}\begin{bmatrix} \dot{\boldsymbol{a}} \\ \dot{\boldsymbol{b}} \end{bmatrix} + \begin{bmatrix} \boldsymbol{X}^T \boldsymbol{K} \boldsymbol{X} + \boldsymbol{\Lambda}(\boldsymbol{X}^T \boldsymbol{M} \boldsymbol{X})\boldsymbol{\Lambda} & \\ & \overline{\boldsymbol{X}}^T \boldsymbol{K} \overline{\boldsymbol{X}} + \overline{\boldsymbol{\Lambda}}\left(\overline{\boldsymbol{X}}^T \boldsymbol{M} \overline{\boldsymbol{X}}\right)\overline{\boldsymbol{\Lambda}} \end{bmatrix}\begin{bmatrix} \boldsymbol{a} \\ \boldsymbol{b} \end{bmatrix} = \begin{bmatrix} \boldsymbol{X}^T \mathbf{p}(t) \\ \overline{\boldsymbol{X}}^T \mathbf{p}(t) \end{bmatrix} \tag{1.13}$$

Accounting for the normalization [1.12a,b), the left side of Eq.(1.13) can be reformulated:

$$\begin{bmatrix}\boldsymbol{\Lambda}-\overline{\boldsymbol{\Lambda}} & \\ & \overline{\boldsymbol{\Lambda}}-\boldsymbol{\Lambda}\end{bmatrix}\begin{bmatrix}\dot{\boldsymbol{a}}\\ \dot{\boldsymbol{b}}\end{bmatrix}+\begin{bmatrix}(\overline{\boldsymbol{\Lambda}}-\boldsymbol{\Lambda})\boldsymbol{\Lambda} & \\ & (\boldsymbol{\Lambda}-\overline{\boldsymbol{\Lambda}})\overline{\boldsymbol{\Lambda}}\end{bmatrix}\begin{bmatrix}\boldsymbol{a}\\ \boldsymbol{b}\end{bmatrix}=\begin{bmatrix}\boldsymbol{X}^T\mathbf{p}(t)\\ \overline{\boldsymbol{X}}^T\mathbf{p}(t)\end{bmatrix} \quad (1.14)$$

The state space form (1.6) is now decoupled in the complex form (1.14). Note that although Eq. (1.6) has been decoupled in state space, the new introduced complex variables $\begin{bmatrix}\boldsymbol{a}\\ \boldsymbol{b}\end{bmatrix}$, see Eq. (1.8), cannot be classified as displacements and velocities.

The next step is to define a purely real 2n-dimensional vector $[\boldsymbol{x}^T \quad \boldsymbol{y}^T]^T$ by

$$\begin{bmatrix}\boldsymbol{x}\\ \boldsymbol{y}\end{bmatrix}=\begin{bmatrix}\boldsymbol{I} & \boldsymbol{I}\\ \boldsymbol{\Lambda} & \overline{\boldsymbol{\Lambda}}\end{bmatrix}\begin{bmatrix}\boldsymbol{a}\\ \boldsymbol{b}\end{bmatrix} \quad (1.15)$$

The inverse relationship of (1.15) is

$$\begin{bmatrix}\boldsymbol{a}\\ \boldsymbol{b}\end{bmatrix}=\begin{bmatrix}\boldsymbol{I} & \boldsymbol{I}\\ \boldsymbol{\Lambda} & \overline{\boldsymbol{\Lambda}}\end{bmatrix}^{-1}\begin{bmatrix}\boldsymbol{x}\\ \boldsymbol{y}\end{bmatrix}=\underbrace{\begin{bmatrix}(\overline{\boldsymbol{\Lambda}}-\boldsymbol{\Lambda})^{-1}\overline{\boldsymbol{\Lambda}} & (\boldsymbol{\Lambda}-\overline{\boldsymbol{\Lambda}})^{-1}\\ (\boldsymbol{\Lambda}-\overline{\boldsymbol{\Lambda}})^{-1}\boldsymbol{\Lambda} & (\overline{\boldsymbol{\Lambda}}-\boldsymbol{\Lambda})^{-1}\end{bmatrix}}_{\boldsymbol{S}}\begin{bmatrix}\boldsymbol{x}\\ \boldsymbol{y}\end{bmatrix}=\boldsymbol{S}\begin{bmatrix}\boldsymbol{x}\\ \boldsymbol{y}\end{bmatrix} \quad (1.16)$$

The reason of the definition (1.15) and its inverse (1.16) is better clarified in Sec. 2, see Eq. (2.16), (2.18), (2.23).

Finally we substitute Eq.(1.16) into (1.14) and then pre-multiply the resulting equation by $\boldsymbol{S}^T$ to obtain the real-space relationship

$$\begin{bmatrix}(\overline{\boldsymbol{\Lambda}}-\boldsymbol{\Lambda})^{-1}(-\overline{\boldsymbol{\Lambda}}\overline{\boldsymbol{\Lambda}}+\boldsymbol{\Lambda}\boldsymbol{\Lambda}) & \boldsymbol{I}\\ \boldsymbol{I} & \mathbf{0}\end{bmatrix}\begin{bmatrix}\dot{\boldsymbol{x}}\\ \dot{\boldsymbol{y}}\end{bmatrix}+\begin{bmatrix}(\overline{\boldsymbol{\Lambda}}-\boldsymbol{\Lambda})^{-1}(\overline{\boldsymbol{\Lambda}}\,\boldsymbol{\Lambda}\,\overline{\boldsymbol{\Lambda}}-\boldsymbol{\Lambda}\,\overline{\boldsymbol{\Lambda}}\,\boldsymbol{\Lambda}) & \mathbf{0}\\ \mathbf{0} & -\boldsymbol{I}\end{bmatrix}\begin{bmatrix}\boldsymbol{x}\\ \boldsymbol{y}\end{bmatrix}=\begin{bmatrix}(\overline{\boldsymbol{\Lambda}}-\boldsymbol{\Lambda})^{-1}(\overline{\boldsymbol{\Lambda}}\boldsymbol{X}^T-\boldsymbol{\Lambda}\overline{\boldsymbol{X}}^T)\,\mathbf{p}(t)\\ (\overline{\boldsymbol{\Lambda}}-\boldsymbol{\Lambda})^{-1}(\overline{\boldsymbol{X}}^T-\boldsymbol{X}^T)\,\mathbf{p}(t)\end{bmatrix}$$

$$\begin{bmatrix}\boldsymbol{D}_1 & \boldsymbol{I}\\ \boldsymbol{I} & \mathbf{0}\end{bmatrix}\begin{bmatrix}\dot{\boldsymbol{x}}\\ \dot{\boldsymbol{y}}\end{bmatrix}+\begin{bmatrix}\boldsymbol{\Omega}_1 & \mathbf{0}\\ \mathbf{0} & -\boldsymbol{I}\end{bmatrix}\begin{bmatrix}\boldsymbol{x}\\ \boldsymbol{y}\end{bmatrix}=\begin{bmatrix}\boldsymbol{T}_1^T\,\mathbf{p}(t)\\ \boldsymbol{T}_2^T\,\mathbf{p}(t)\end{bmatrix} \quad (1.17)$$

where $\boldsymbol{D}_1, \boldsymbol{\Omega}_1, \boldsymbol{T}_1$ and $\boldsymbol{T}_2$ are real-space matrices (what can easy be checked):

$$\boldsymbol{D}_1=(\overline{\boldsymbol{\Lambda}}-\boldsymbol{\Lambda})^{-1}(-\overline{\boldsymbol{\Lambda}}\overline{\boldsymbol{\Lambda}}+\boldsymbol{\Lambda}\boldsymbol{\Lambda})=-diag[\lambda_1+\bar{\lambda}_1,\cdots,\lambda_j+\bar{\lambda}_j,\cdots,\lambda_n+\bar{\lambda}_n]=-diag[2\alpha_1,\cdots,2\alpha_j,\cdots,2\alpha_n] \quad (1.18)$$

$$\boldsymbol{\Omega}_1=(\overline{\boldsymbol{\Lambda}}-\boldsymbol{\Lambda})^{-1}(\overline{\boldsymbol{\Lambda}}\,\boldsymbol{\Lambda}\,\overline{\boldsymbol{\Lambda}}-\boldsymbol{\Lambda}\,\overline{\boldsymbol{\Lambda}}\,\boldsymbol{\Lambda})=diag[\lambda_1\bar{\lambda}_1,\cdots,\lambda_j\bar{\lambda}_j,\cdots,\lambda_n\bar{\lambda}_n]=diag[\alpha_1^2+\omega_{D1}^2,\cdots,\alpha_j^2+\omega_{Dj}^2,\cdots,\alpha_n^2+\omega_{Dn}^2] \quad (1.19)$$

$$\boldsymbol{T}_1=(\boldsymbol{X}\overline{\boldsymbol{\Lambda}}-\overline{\boldsymbol{X}}\boldsymbol{\Lambda})(\overline{\boldsymbol{\Lambda}}-\boldsymbol{\Lambda})^{-1} \quad (1.20)$$

$$\boldsymbol{T}_2=(\overline{\boldsymbol{X}}-\boldsymbol{X})(\overline{\boldsymbol{\Lambda}}-\boldsymbol{\Lambda})^{-1} \quad (1.21)$$

The upper and lower halves of the final uncoupled equations (1.17) are

$$\dot{\boldsymbol{y}}+\boldsymbol{D}_1\dot{\boldsymbol{x}}+\boldsymbol{\Omega}_1\boldsymbol{x}=\boldsymbol{T}_1^T\,\mathbf{p}(t) \quad (1.22)$$

$$\dot{\boldsymbol{x}}-\boldsymbol{y}=\boldsymbol{T}_2^T\,\mathbf{p}(t) \quad (1.23)$$

Expressing $\boldsymbol{y}$ from (1.23) and replacing it in (1.22) we get

$$\ddot{\boldsymbol{x}}+\boldsymbol{D}_1\dot{\boldsymbol{x}}+\boldsymbol{\Omega}_1\boldsymbol{x}=\boldsymbol{T}_1^T\,\mathbf{p}(t)+\boldsymbol{T}_2^T\,\dot{\mathbf{p}}(t) \quad (1.24)$$

Eq. (1.24) is the transformed uncoupled real-space form of the original equations of motion (1.1), the introduced n-dimensional vector $\boldsymbol{x}$ can be referred to as modal coordinates. The relationship between the modal coordinates $\boldsymbol{x}$ and the solution original $\mathbf{V}$ of the original system (1.1) can be derived by combining the first complex transformation (1.8) with the complex transformation introduced by (1.15):

$$\begin{bmatrix}\boldsymbol{V}\\ \dot{\boldsymbol{V}}\end{bmatrix} = \begin{bmatrix}\boldsymbol{X} & \overline{\boldsymbol{X}}\\ \boldsymbol{X}\,\boldsymbol{\Lambda} & \overline{\boldsymbol{X}}\,\overline{\boldsymbol{\Lambda}}\end{bmatrix}\begin{bmatrix}\boldsymbol{a}\\ \boldsymbol{b}\end{bmatrix} = \begin{bmatrix}\boldsymbol{X} & \overline{\boldsymbol{X}}\\ \boldsymbol{X}\,\boldsymbol{\Lambda} & \overline{\boldsymbol{X}}\,\overline{\boldsymbol{\Lambda}}\end{bmatrix}\begin{bmatrix}\boldsymbol{I} & \boldsymbol{I}\\ \boldsymbol{\Lambda} & \overline{\boldsymbol{\Lambda}}\end{bmatrix}^{-1}\begin{bmatrix}\boldsymbol{x}\\ \boldsymbol{y}\end{bmatrix} \tag{1.25}$$

The upper half of (1.25) is

$$\boldsymbol{V} = \left(\boldsymbol{X}\overline{\boldsymbol{\Lambda}} - \overline{\boldsymbol{X}}\boldsymbol{\Lambda}\right)\left(\overline{\boldsymbol{\Lambda}} - \boldsymbol{\Lambda}\right)^{-1}\boldsymbol{x} + \left(\overline{\boldsymbol{X}} - \boldsymbol{X}\right)\left(\overline{\boldsymbol{\Lambda}} - \boldsymbol{\Lambda}\right)^{-1}\boldsymbol{y} = \boldsymbol{T_1}\boldsymbol{x} + \boldsymbol{T_2}\boldsymbol{y} \tag{1.26a}$$

and, accounting for Eq.(1.23):

$$\boldsymbol{V} = \boldsymbol{T_1}\boldsymbol{x} + \boldsymbol{T_2}\left(\dot{\boldsymbol{x}} - \boldsymbol{T}_2^T\,\mathbf{p}(t)\right) \tag{1.26b}$$

By use of Eq.(1.23) the real-space solution (1.25) can be rewritten in state space

$$\begin{bmatrix}\boldsymbol{V}(t)\\ \dot{\boldsymbol{V}}(t)\end{bmatrix} = \begin{bmatrix}\boldsymbol{X} & \overline{\boldsymbol{X}}\\ \boldsymbol{X}\,\boldsymbol{\Lambda} & \overline{\boldsymbol{X}}\,\overline{\boldsymbol{\Lambda}}\end{bmatrix}\begin{bmatrix}\boldsymbol{I} & \boldsymbol{I}\\ \boldsymbol{\Lambda} & \overline{\boldsymbol{\Lambda}}\end{bmatrix}^{-1}\begin{bmatrix}\boldsymbol{x}(t)\\ \dot{\boldsymbol{x}}(t) - \boldsymbol{T}_2^T\,\mathbf{p}(t)\end{bmatrix} \tag{1.27}$$

The inverse transformation is

$$\begin{bmatrix}\boldsymbol{x}(t)\\ \dot{\boldsymbol{x}}(t)\end{bmatrix} = \begin{bmatrix}\boldsymbol{I} & \boldsymbol{I}\\ \boldsymbol{\Lambda} & \overline{\boldsymbol{\Lambda}}\end{bmatrix}\begin{bmatrix}\boldsymbol{X} & \overline{\boldsymbol{X}}\\ \boldsymbol{X}\,\boldsymbol{\Lambda} & \overline{\boldsymbol{X}}\,\overline{\boldsymbol{\Lambda}}\end{bmatrix}^{-1}\begin{bmatrix}\boldsymbol{V}(t)\\ \dot{\boldsymbol{V}}(t)\end{bmatrix} + \begin{bmatrix}\boldsymbol{0}\\ \boldsymbol{T}_2^T\,\mathbf{p}(t)\end{bmatrix} \tag{1.28}$$

2 MODAL TRANSFORMATION PROCEDURE BASED ON THE COMPLEX RIGHT EIGENVECTORS

2.1 Complex modal transformation of the MDOFS equations

In this section is described a procedure, similar to the phase synchronization method in state space formulation, presented in Section 1. We will consider the case of forced vibrations with n distinct complex conjugated eigenvalues λ_j, see Eq. (2.3), what is the most relevant case in structural mechanics based on finite element formulation.

The detailed development of the procedure differs in some points from the decomposition method based on the *Lancaster form* (1.6). The description of the differences in details, compared to the development steps in Section 1, aims to outline the structural mechanics background of the utilized mathematical transformations.

At first the equations of motion (1.1) are recast to first order equations in state space:

$$\underbrace{\begin{bmatrix}\boldsymbol{M} & \\ & -\boldsymbol{K}\end{bmatrix}}_{\boldsymbol{M_G}}\underbrace{\begin{bmatrix}\ddot{\boldsymbol{V}}\\ \dot{\boldsymbol{V}}\end{bmatrix}}_{\dot{\boldsymbol{Q}}} + \underbrace{\begin{bmatrix}\boldsymbol{D} & \boldsymbol{K}\\ \boldsymbol{K} & \end{bmatrix}}_{\boldsymbol{K_G}}\underbrace{\begin{bmatrix}\dot{\boldsymbol{V}}\\ \boldsymbol{V}\end{bmatrix}}_{\boldsymbol{Q}} = \underbrace{\begin{bmatrix}\boldsymbol{p}(t)\\ \\ \end{bmatrix}}_{\boldsymbol{P}} \tag{2.1}$$

where $\boldsymbol{M_G}$ and $\boldsymbol{K_G}$ are, respectively the (2n x 2n) symmetric generalized mass and the generalized stiffness matrices. The formulation in state space (2.1) doesn't use the Lancaster form (1.7a), but retains the symmetry in the generalized matrices.

The associated quadratic eigenvalue problem can be written in the 2n-dimensional form

$$\left(\lambda^{(j)}\boldsymbol{M_G} + \boldsymbol{K_G}\right)\begin{bmatrix}\lambda^{(j)}\boldsymbol{X}^{(j)}\\ \boldsymbol{X}^{(j)}\end{bmatrix} = \boldsymbol{0} \tag{2.2}$$

where

$$\lambda^{(j)} = \lambda_r^{(j)} + i\lambda_i^{(j)} \rightarrow \begin{bmatrix} \lambda^{(j)}\boldsymbol{X}^{(j)} \\ \boldsymbol{X}^{(j)} \end{bmatrix}, \qquad \overline{\lambda}^{(j)} = \lambda_r^{(j)} - i\lambda_i^{(j)} \rightarrow \begin{bmatrix} \overline{\lambda}^{(j)}\overline{\boldsymbol{X}}^{(j)} \\ \overline{\boldsymbol{X}}^{(j)} \end{bmatrix}, (j = 1, \dots, n) \quad (2.3)$$

are the corresponding n complex conjugate eigenpairs.

Each j[th] eigenvector-pair $\boldsymbol{X}^{(j)}, \overline{\boldsymbol{X}}^{(j)}$ can be normalized (index (j) omitted) with respect to the general mass matrix $\boldsymbol{M_G}$:

$$\begin{bmatrix} \lambda\boldsymbol{X} \\ \boldsymbol{X} \end{bmatrix}^T \begin{bmatrix} \boldsymbol{M} & \\ & -\boldsymbol{K} \end{bmatrix} \begin{bmatrix} \lambda\boldsymbol{X} \\ \boldsymbol{X} \end{bmatrix} = A + iB \quad \rightarrow \boldsymbol{\Phi} = \frac{\boldsymbol{X}}{\sqrt{A+iB}} = \boldsymbol{\Phi_r} + i\boldsymbol{\Phi_i} \qquad (2.4a)$$

$$\begin{bmatrix} \overline{\lambda\boldsymbol{X}} \\ \overline{\boldsymbol{X}} \end{bmatrix}^T \begin{bmatrix} \boldsymbol{M} & \\ & -\boldsymbol{K} \end{bmatrix} \begin{bmatrix} \overline{\lambda\boldsymbol{X}} \\ \overline{\boldsymbol{X}} \end{bmatrix} = A - iB \quad \rightarrow \overline{\boldsymbol{\Phi}} = \frac{\overline{\boldsymbol{X}}}{\sqrt{A-iB}} = \boldsymbol{\Phi_r} - i\boldsymbol{\Phi_i} \qquad (2.4b)$$

The mass normalization (2.4) leads to the orthogonality relationships (2.5), (2.6) - expressed in terms of the j[th] eigenvector-pair (index (j) omitted):

$$\begin{bmatrix} \lambda\boldsymbol{\Phi} & \overline{\lambda\boldsymbol{\Phi}} \\ \boldsymbol{\Phi} & \overline{\boldsymbol{\Phi}} \end{bmatrix}^T \begin{bmatrix} \boldsymbol{M} & \\ & -\boldsymbol{K} \end{bmatrix} \begin{bmatrix} \lambda\boldsymbol{\Phi} & \overline{\lambda\boldsymbol{\Phi}} \\ \boldsymbol{\Phi} & \overline{\boldsymbol{\Phi}} \end{bmatrix} = \begin{bmatrix} 1 & \\ & 1 \end{bmatrix} \qquad (2.5)$$

$$\begin{bmatrix} \lambda\boldsymbol{\Phi} & \overline{\lambda\boldsymbol{\Phi}} \\ \boldsymbol{\Phi} & \overline{\boldsymbol{\Phi}} \end{bmatrix}^T \begin{bmatrix} \boldsymbol{D} & \boldsymbol{K} \\ \boldsymbol{K} & \end{bmatrix} \begin{bmatrix} \lambda\boldsymbol{\Phi} & \overline{\lambda\boldsymbol{\Phi}} \\ \boldsymbol{\Phi} & \overline{\boldsymbol{\Phi}} \end{bmatrix} = \begin{bmatrix} -\lambda & \\ & -\overline{\lambda} \end{bmatrix} \qquad (2.6)$$

Then the (2n x 2n) complex modal matrix $\boldsymbol{\Phi_G}$ can be built up:

$$\boldsymbol{\Phi_G} = \begin{bmatrix} \lambda^{(1)}\boldsymbol{\Phi}^{(1)} & \overline{\lambda}^{(1)}\overline{\boldsymbol{\Phi}}^{(1)} & \cdots & \lambda^{(n)}\boldsymbol{\Phi}^{(n)} & \overline{\lambda}^{(n)}\overline{\boldsymbol{\Phi}}^{(n)} \\ \boldsymbol{\Phi}^{(1)} & \overline{\boldsymbol{\Phi}}^{(1)} & \cdots & \boldsymbol{\Phi}^{(n)} & \overline{\boldsymbol{\Phi}}^{(n)} \end{bmatrix} \qquad (2.7)$$

Note the difference to the form of Eq. (1.8), (1.9) - the complex eigenvectors $\boldsymbol{X}$ and the conjugated complex $\overline{\boldsymbol{X}}$ are split, but in (2.7) they are in pairs.

Complex modal decomposition of the equations of motion (2.1) can be performed by use of the orthogonality relationships (2.5), (2.6):

$$\underbrace{\boldsymbol{\Phi_G^T} \begin{bmatrix} \boldsymbol{M} & \\ & -\boldsymbol{K} \end{bmatrix} \boldsymbol{\Phi_G}}_{\begin{bmatrix} 1 & & \\ & \cdots & \\ & & 1 \end{bmatrix}} \cdot \dot{\boldsymbol{A}} + \underbrace{\boldsymbol{\Phi_G^T} \begin{bmatrix} \boldsymbol{D} & \boldsymbol{K} \\ \boldsymbol{K} & \end{bmatrix} \boldsymbol{\Phi_G}}_{\begin{bmatrix} -\lambda^{(1)} & & & & \\ & -\overline{\lambda}^{(1)} & & & \\ & & \cdots & & \\ & & & -\lambda^{(n)} & \\ & & & & -\overline{\lambda}^{(n)} \end{bmatrix}} \cdot \boldsymbol{A} = \underbrace{\boldsymbol{\Phi_G^T} \begin{bmatrix} \boldsymbol{p}(t) \end{bmatrix}}_{\begin{bmatrix} \lambda^{(1)}\left(\boldsymbol{\Phi}^{(1)}\right)^T\boldsymbol{p} \\ \overline{\lambda}^{(1)}\left(\overline{\boldsymbol{\Phi}}^{(1)}\right)^T\boldsymbol{p} \\ \cdots \\ \lambda^{(n)}\left(\boldsymbol{\Phi}^{(n)}\right)^T\boldsymbol{p} \\ \overline{\lambda}^{(n)}\left(\overline{\boldsymbol{\Phi}}^{(n)}\right)^T\boldsymbol{p} \end{bmatrix}} \qquad (2.8)$$

where the new complex modal coordinates $\mathbf{A}$ are introduced by Eq. (2.9):

$$\begin{bmatrix} \dot{\boldsymbol{V}} \\ \boldsymbol{V} \end{bmatrix} = \boldsymbol{\Phi_G}\,\boldsymbol{A}(t) = \boldsymbol{\Phi_G}\left[a^{(1)}(t) \quad b^{(1)}(t) \quad \cdots \quad a^{(n)}(t) \quad b^{(n)}(t)\right]^{\boldsymbol{T}} \qquad (2.9)$$

According to the assembly of the global modal matrix $\boldsymbol{\Phi_G}$ in (2.7) the complex coordinates $a^{(j)}, b^{(j)}$ in the definition (2.9) remain in pairs, corresponding to the eigenvalue pair $(\lambda^{(j)}, \overline{\lambda}^{(j)}$, whereas in the definition (1.8) in Section 1 they are separated. In comparison to the analogous decoupling transformation (1.14) the uncoupled modal equations (2.8) have - due to the mass normalization (2.4) - a very clear and more simple form of the modal mass matrix (equal to the unity matrix) and of the modal stiffness matrix (equal to the spectral matrix).

In a next step a second transformation of the complex modal equations (2.8) will be introduced in order to get $(j = 1, \ldots, n)$ uncoupled single oscillator equations in real space. To explain better this step, the equation of a single- degree-of-freedom system (SDOFS) is considered in the next section.

2.2 The single mass oscillator equation

The equation of motion of a viscously damped single degree of freedom system (SDOFS)

$$m\ddot{v}(t) + c\dot{v}(t) + kv(t) = q(t) \tag{2.10}$$

can be written in the extended form

$$\underbrace{\begin{bmatrix} 1 & \\ & -\omega^2 \end{bmatrix}}_{\boldsymbol{m}} \underbrace{\begin{bmatrix} \ddot{v}(t) \\ \dot{v}(t) \end{bmatrix}}_{\dot{\boldsymbol{q}}} + \underbrace{\begin{bmatrix} 2\eta\omega & \omega^2 \\ \omega^2 & \end{bmatrix}}_{\boldsymbol{k}} \underbrace{\begin{bmatrix} \dot{v}(t) \\ v(t) \end{bmatrix}}_{\boldsymbol{q}} = \underbrace{\begin{bmatrix} p(t) \\ \end{bmatrix}}_{\boldsymbol{p}} \qquad \leftarrow \boldsymbol{q} = \begin{bmatrix} \dot{v}(t) \\ v(t) \end{bmatrix}$$

$$\boldsymbol{m}\dot{\boldsymbol{q}} + \boldsymbol{k}\boldsymbol{q} = \boldsymbol{p} \tag{2.11}$$

where $\ddot{v}$ is acceleration, $\dot{v}$ - velocity, $v(t)$ - displacement, $\omega = \sqrt{\frac{k}{m}}$ - free vibration frequency, $\eta = \frac{c}{2m\omega}$ - Lehr's damping ratio and $p(t) = \frac{q(t)}{m}$.

Introducing the exponential approach $\boldsymbol{q} = \boldsymbol{x}e^{\lambda t}$ and the (2 x 2) matrix $\boldsymbol{a}$

$$\boldsymbol{a} = \boldsymbol{m}^{-1}\boldsymbol{k} \tag{2.12}$$

into the homogenous form of the differential equation (2.11) leads to the quadratic eigenvalue problem

$$\dot{\boldsymbol{q}} + \underbrace{(\boldsymbol{m}^{-1}\boldsymbol{k})}_{\boldsymbol{a}}\,\boldsymbol{q} = \boldsymbol{0} \qquad \rightarrow \qquad (\boldsymbol{a} + \lambda_j \boldsymbol{e})\boldsymbol{r}_j = \boldsymbol{0} \quad (j = 1{,}2) \tag{2.13}$$

The solution are two complex conjugate eigenvalues ($\eta \ll 1$, subcritical damped system):

$$\left.\begin{aligned} \lambda &= \lambda_r + i\lambda_i = \alpha + i\omega_D \\ \bar{\lambda} &= \lambda_r - i\lambda_i = \alpha - i\omega_D \end{aligned}\right\} \quad \text{where} \quad \lambda_r = -\eta\omega = \alpha\,, \quad \lambda_i = \omega\sqrt{1-\eta^2} = \omega_D \tag{2.14}$$

The natural frequency ω and the damping ratio η can be determined from (2.14) to

$$\omega = \sqrt{(\lambda_r)^2 + (\lambda_i)^2}\,, \qquad \eta = -\frac{\lambda_r}{\omega} \tag{2.15a,b}$$

The corresponding complex conjugate right eigenvectors in Eq. (2.13) are

$$\boldsymbol{r}_j = \begin{bmatrix} \lambda_r \pm i\lambda_i \\ 1 \end{bmatrix} \qquad (j = 1{,}2) \tag{2.16}$$

After normalization of the eigenvectors with respect to the mass matrix

$$[\boldsymbol{r}_1 \quad \boldsymbol{r}_2]^T \cdot \boldsymbol{m} \cdot [\boldsymbol{r}_1 \quad \boldsymbol{r}_2] = \begin{bmatrix} g_1 & \\ & g_2 \end{bmatrix} \qquad \rightarrow \boldsymbol{\varphi}_j = \frac{r_j}{\sqrt{g_j}} \qquad (j = 1{,}2) \tag{2.17}$$

the (2 x 2) modal matrix $\boldsymbol{\varphi}$ is cast:

$$\boldsymbol{\varphi} = [\boldsymbol{\varphi}_1 \quad \boldsymbol{\varphi}_2] \tag{2.18}$$

The mass normalization (2.17) leads to orthogonality relations and their inverse relationships:

$$\boldsymbol{\varphi}^T \boldsymbol{m}\, \boldsymbol{\varphi} = \boldsymbol{\varphi}^T \begin{bmatrix} 1 & \\ & -\omega^2 \end{bmatrix} \boldsymbol{\varphi} = \begin{bmatrix} 1 & \\ & 1 \end{bmatrix} \leftrightarrow (\boldsymbol{\varphi}^T)^{-1} \begin{bmatrix} 1 & \\ & 1 \end{bmatrix} \boldsymbol{\varphi}^{-1} = \begin{bmatrix} 1 & \\ & -\omega^2 \end{bmatrix} \quad 2.19)$$

$$\boldsymbol{\varphi}^T \boldsymbol{k}\, \boldsymbol{\varphi} = \boldsymbol{\varphi}^T \begin{bmatrix} 2\eta\omega & \omega^2 \\ \omega^2 & \end{bmatrix} \boldsymbol{\varphi} = \begin{bmatrix} -\lambda & \\ & -\bar{\lambda} \end{bmatrix} \leftrightarrow (\boldsymbol{\varphi}^T)^{-1} \begin{bmatrix} -\lambda & \\ & -\bar{\lambda} \end{bmatrix} \boldsymbol{\varphi}^{-1} = \begin{bmatrix} 2\eta\omega & \omega^2 \\ \omega^2 & \end{bmatrix} \quad (2.20)$$

The inverse of the complex modal matrix $\boldsymbol{\varphi}(\omega, \eta)$ can be expressed analytically by the aid of computer algebra software - see Eq. (2.21), (2.22a,b).

$$\boldsymbol{\varphi}^{-1} = \frac{1}{2\sqrt{1-\eta^2}} \begin{bmatrix} -Z_1 - iZ_2 & P - iQ \\ -Z_1 + iZ_2 & P + iQ \end{bmatrix} \quad (2.21)$$

where

$$Z_1 = \sqrt{\sqrt{1-\eta^2} + (1-\eta^2)} \qquad Z_2 = \sqrt{\sqrt{1-\eta^2} - (1-\eta^2)} \quad (2.22a)$$

$$P = \omega\left(Z_2\sqrt{1-\eta^2} - Z_1\eta\right) \qquad Q = \omega\left(Z_1\sqrt{1-\eta^2} + Z_2\eta\right) \quad (2.22b)$$

2.3 Final decomposition of the MDOFS equations in real space

We come back to the uncoupled complex modal equations (2.8). Here the complex modal coordinates $[a^{(j)} \quad b^{(j)}]^T$, see Eq. (2.9), will be replaced by new real coordinates $[x^{(j)} \quad y^{(j)}]^T$ for each j-th eigenpair, introduced by the definition (2.23):

$$\begin{bmatrix} a^{(j)}(t) \\ b^{(j)}(t) \end{bmatrix} = \left(\boldsymbol{\varphi}^{(j)}\right)^{-1} \begin{bmatrix} x^{(j)}(t) \\ y^{(j)}(t) \end{bmatrix}, \qquad \begin{bmatrix} \dot{a}^{(j)} \\ \dot{b}^{(j)} \end{bmatrix} = \left(\boldsymbol{\varphi}^{(j)}\right)^{-1} \begin{bmatrix} \dot{x}^{(j)} \\ \dot{y}^{(j)} \end{bmatrix} \quad (2.23)$$

Taking into account (2.23), the modal equations (2.8) can be transformed **in pairs** into the real form of SDOFS-equation (index (j) omitted), with regard to the inverse relationships (2.19), (2.20):

$$\underbrace{(\boldsymbol{\varphi}^T)^{-1} \begin{bmatrix} 1 & \\ & 1 \end{bmatrix} \boldsymbol{\varphi}^{-1}}_{\begin{bmatrix} 1 & \\ & -\omega^2 \end{bmatrix}} \cdot \begin{bmatrix} \dot{x} \\ \dot{y} \end{bmatrix} + \underbrace{(\boldsymbol{\varphi}^T)^{-1} \begin{bmatrix} -\lambda & \\ & -\bar{\lambda} \end{bmatrix} \boldsymbol{\varphi}^{-1}}_{\begin{bmatrix} 2\eta\omega & \omega^2 \\ \omega^2 & \end{bmatrix}} \cdot \begin{bmatrix} x \\ y \end{bmatrix} = \underbrace{(\boldsymbol{\varphi}^T)^{-1} \begin{bmatrix} \lambda \boldsymbol{\Phi}^T \boldsymbol{p}(t) \\ \bar{\lambda} \bar{\boldsymbol{\Phi}}^T \boldsymbol{p}(t) \end{bmatrix}}_{\begin{bmatrix} g(t) \\ h(t) \end{bmatrix}} \quad (2.24)$$

Note that the matrix $\left(\boldsymbol{\varphi}^{(j)}\right)^{-1}$ can be expressed according to Eq. (2.21), (2.15a,b) simply by the real and imaginary parts $\lambda_r^{(j)}, \lambda_i^{(j)}$.

Combining the two complex transformations (2.8) and (2.24), a new (2n x 2n) transformation basis $\boldsymbol{Y}$ can be defined:

$$\begin{bmatrix} \dot{\boldsymbol{V}} \\ \boldsymbol{V} \end{bmatrix} = \begin{bmatrix} \lambda^{(1)}\boldsymbol{\Phi}^{(1)} & \bar{\lambda}^{(1)}\bar{\boldsymbol{\Phi}}^{(1)} & \cdots & \lambda^{(n)}\boldsymbol{\Phi}^{(n)} & \bar{\lambda}^{(n)}\bar{\boldsymbol{\Phi}}^{(n)} \\ \boldsymbol{\Phi}^{(1)} & \bar{\boldsymbol{\Phi}}^{(1)} & \cdots & \boldsymbol{\Phi}^{(n)} & \bar{\boldsymbol{\Phi}}^{(n)} \end{bmatrix} \underbrace{\begin{bmatrix} \left(\boldsymbol{\varphi}^{(1)}\right)^{-1} & & \\ & \cdots & \\ & & \left(\boldsymbol{\varphi}^{(n)}\right)^{-1} \end{bmatrix}}_{\boldsymbol{\Psi}^{-1}} \underbrace{\begin{bmatrix} x^{(1)} \\ y^{(1)} \\ \cdots \\ x^{(n)} \\ y^{(n)} \end{bmatrix}}_{\boldsymbol{X}} = \underbrace{\boldsymbol{\Phi}_G \cdot \boldsymbol{\Psi}^{-1}}_{\boldsymbol{Y}} \cdot \boldsymbol{X}$$

$$\begin{bmatrix} \dot{\boldsymbol{V}} \\ \boldsymbol{V} \end{bmatrix} = \boldsymbol{Y} \cdot \boldsymbol{X} \quad (2.25)$$

By the aid of the transformation (2.25) and with regard to (2.8) and (2.24), the equations of motion (2.1) can be decomposed into n real uncoupled SDOFS block equations as follows:

$$\underbrace{\boldsymbol{Y}^T\cdot\begin{bmatrix}\boldsymbol{M} & \\ & -\boldsymbol{K}\end{bmatrix}\cdot\boldsymbol{Y}}_{\begin{bmatrix}1 & & & & \\ & -\omega_1^2 & & & \\ & & \cdots & & \\ & & & 1 & \\ & & & & -\omega_n^2\end{bmatrix}}\cdot\underbrace{\begin{bmatrix}\dot{x}^{(1)}\\ \dot{y}^{(1)}\\ \cdots\\ \dot{x}^{(n)}\\ \dot{y}^{(n)}\end{bmatrix}}_{\dot{\boldsymbol{X}}}+\underbrace{\boldsymbol{Y}^T\cdot\begin{bmatrix}\boldsymbol{D} & \boldsymbol{K}\\ \boldsymbol{K} & \end{bmatrix}\cdot\boldsymbol{Y}}_{\begin{bmatrix}2\eta_1\,\omega_1 & \omega_1^2 & & & \\ \omega_1^2 & 0 & & & \\ & & \cdots & & \\ & & & 2\eta_n\,\omega_n & \omega_n^2\\ & & & \omega_n^2 & 0\end{bmatrix}}\cdot\underbrace{\begin{bmatrix}x^{(1)}\\ y^{(1)}\\ \cdots\\ x^{(n)}\\ y^{(n)}\end{bmatrix}}_{\boldsymbol{X}}=\underbrace{\boldsymbol{Y}^T\cdot\begin{bmatrix}\boldsymbol{p}\\ \end{bmatrix}}_{\begin{bmatrix}g_1\\ h_1\\ \cdots\\ g_n\\ h_n\end{bmatrix}} \qquad (2.26)$$

It can be shown that the $\boldsymbol{Y}$-matrix and all „load“-vectors $[g(t) \quad h(t)]^T$ in Eq. (2.26) are purely real. In (E. Stanoev, 2013, 2014) has been shown that after component multiplication of the analytically expressed terms of $\boldsymbol{\Phi_G}$ and of $\boldsymbol{\Psi^{-1}}$ all imaginary parts cancel each other.

The transformation in Section 1, analogously to (2.23), is given by Eq. (1.16). The advantage of the (2 x 2) transformation used in (2.24) is that it is done on the level “SDOFS-equation”, employing mass normalization for the modal matrix $\boldsymbol{\varphi}$ - see Eq.(2.17). In contrast to this in the relationship (1.16) a (2n x 2n) matrix $\begin{bmatrix}\boldsymbol{I} & \boldsymbol{I}\\ \boldsymbol{\Lambda} & \bar{\boldsymbol{\Lambda}}\end{bmatrix}$ has to be inverted. Besides the analytical inversion of the simple (2 x 2) matrix $\boldsymbol{\varphi}^{(j)}$ in (2.21), the definition (2.23) seems quite natural in order to transform the complex modal equations (2.8) back to the real form of SDOFS - as seen in (2.24).

The mechanical reason of the relationship (1.16) and the inverse form (1.15) is clarified by looking at the eigenvectors (2.16) of the SDOFS. Due to the inverse order of displacements and velocities $\begin{bmatrix}\boldsymbol{V}\\ \dot{\boldsymbol{V}}\end{bmatrix}$ in the Lancaster form (1.6) in compare to the formulation (2.1) the meaning of the modal coordinates $x^{(j)}, y^{(j)}$ here is interchanged, compare Eq. (1.24) and (2.28).

Each SDOFS block equation in (2.26) can be solved eliminating the modal coordinate $x^{(j)}$ to obtain the usual form of the SDOFS equation of motion (index (j) omitted):

$$x(t) = \dot{y} + \frac{1}{\omega^2}h(t) \qquad (2.27)$$

$$\ddot{y}(t) + 2\eta\omega\,\dot{y}(t) + \omega^2 y(t) = g(t) - \frac{2\eta}{\omega}h(t) - \frac{1}{\omega^2}\dot{h}(t) \qquad (2.28)$$

A usual numerical step-by-step integration of Eq. (2.28) yields the modal response $y^{(j)}(t)$. The final time series of the original 2n state variables $\begin{bmatrix}\dot{\boldsymbol{V}}\\ \boldsymbol{V}\end{bmatrix}$ are calculated by superposition of the modal coordinates $x^{(j)}, y^{(j)}$ (assembled in $\boldsymbol{X}$) in accordance to Eq. (2.25).

The final SDOFS equations from type (2.28) for each j-th eigenpair can be rebuild in the uncoupled diagonal form (1.24) for the MDOFS - note that $y(t)$ in (2.28) corresponds to $\mathrm{x}(t)$ in (1.24). The right sides of both equations clearly correspond to each other.

2.4 Analytical form of the uncoupled equation system

We introduce a notation of two columns, belonging to each j[th] eigenvector-pair in the real (2n x 2n) matrix $\boldsymbol{Y}$, defined in Eq. (2.25):

$$\boldsymbol{Y} = \begin{bmatrix} \cdots & \boldsymbol{Y}_{x1}^{(j)} & \boldsymbol{Y}_{y1}^{(j)} & \cdots \\ \cdots & \boldsymbol{Y}_{x2}^{(j)} & \boldsymbol{Y}_{y2}^{(j)} & \cdots \end{bmatrix} \tag{2.29}$$

The analytical expressions for (2.29) can be derived using Eq. (2.4), (2.7), (2.21) and (2.22a,b), index (j) omitted:

$$\boldsymbol{Y}_{x1}^{(j)} = \frac{1}{\sqrt{1-\eta^2}}\left\{\left(Z_2\,\omega\sqrt{1-\eta^2} + \eta\omega Z_1\right)\boldsymbol{\Phi_r} + \left(Z_1\,\omega\sqrt{1-\eta^2} - \eta\omega Z_2\right)\boldsymbol{\Phi_i}\right\}$$

$$\boldsymbol{Y}_{x2}^{(j)} = \frac{1}{\sqrt{1-\eta^2}}(-Z_1\boldsymbol{\Phi_r} + Z_2\boldsymbol{\Phi_i}) \tag{2.30a-b}$$

$$\boldsymbol{Y}_{y1}^{(j)} = \frac{1}{\sqrt{1-\eta^2}}(\omega^2 Z_1\boldsymbol{\Phi_r} - \omega^2 Z_2\boldsymbol{\Phi_i})$$

$$\boldsymbol{Y}_{y2}^{(j)} = \frac{1}{\sqrt{1-\eta^2}}\left\{\left(Z_2\,\omega\sqrt{1-\eta^2} - \eta\omega Z_1\right)\boldsymbol{\Phi_r} + \left(Z_1\,\omega\sqrt{1-\eta^2} + \eta\omega Z_2\right)\boldsymbol{\Phi_i}\right\} \tag{2.30c-d}$$

The two components of the associated j^{th} "load" vector, defined in Eq. (2.26), are purely real too:

$$g_j(t) = \frac{\omega}{\sqrt{1-\eta^2}}\left\{\left(Z_2\sqrt{1-\eta^2} + Z_1\eta\right)\boldsymbol{\Phi}_{\boldsymbol{r}}^T + \left(Z_1\sqrt{1-\eta^2} - Z_2\,\eta\right)\boldsymbol{\Phi}_{\boldsymbol{i}}^T\right\}\boldsymbol{p}(t) \tag{2.31a}$$

$$h_j(t) = \frac{\omega^2}{\sqrt{1-\eta^2}}\left\{Z_1\boldsymbol{\Phi}_{\boldsymbol{r}}^T - Z_2\,\boldsymbol{\Phi}_{\boldsymbol{i}}^T\right\}\boldsymbol{p}(t) \tag{2.31b}$$

3 MODAL TRANSFORMATION PROCEDURE BASED ON BOTH COMPLEX RIGHT AND LEFT EIGENVECTORS

3.1 Complex modal decomposition of MDOFS equations with non-modal damping

Here is presented a variant of a modal decomposition method, operating with right and left complex eigenvectors of the $\boldsymbol{A}$-matrix - see Eq. (3.2a), (3.3). The procedure has been first presented in details in (E. Stanoev, 2017). Here is given a briefly description.

The state-space form of equations of motion (2.1) is transformed in two variants using the substitution

$$\boldsymbol{F} = \begin{bmatrix} \boldsymbol{D} & \boldsymbol{K} \\ \boldsymbol{K} & \end{bmatrix}\begin{bmatrix} \dot{\boldsymbol{V}} \\ \boldsymbol{V} \end{bmatrix} = \boldsymbol{K_G Q}\,, \qquad \dot{\boldsymbol{F}} = \boldsymbol{K_G}\dot{\boldsymbol{Q}} \tag{3.1}$$

1^{th} variant: $\dot{\boldsymbol{Q}} + \underbrace{\boldsymbol{M_G^{-1}}\,\boldsymbol{K_G}}_{\boldsymbol{A}}\,\boldsymbol{Q} = \boldsymbol{M_G^{-1}}\,\boldsymbol{P}$

2^{th} variant:

$$\begin{aligned} \underbrace{\boldsymbol{K_G}\,\dot{\boldsymbol{Q}}}_{\dot{\boldsymbol{F}}} \;&+\; \boldsymbol{K_G}\,\boldsymbol{M_G^{-1}}\,\underbrace{(\boldsymbol{K_G}\,\boldsymbol{Q})}_{} &= \boldsymbol{K_G}\,\boldsymbol{M_G^{-1}}\,\boldsymbol{P} \\ \dot{\boldsymbol{F}} \;&+\; \boldsymbol{K_G}\,\boldsymbol{M_G^{-1}}\,\boldsymbol{F} &= \boldsymbol{K_G}\,\boldsymbol{M_G^{-1}}\,\boldsymbol{P} \end{aligned} \tag{3.2a,b}$$

With the notation

$$\boldsymbol{A} = \boldsymbol{M_G^{-1}}\,\boldsymbol{K_G} \tag{3.3}$$

and due to the symmetry of $\boldsymbol{K_G}$ and $\boldsymbol{M_G}$ the relationship (3.4) hold:

$$\boldsymbol{K_G}\,\boldsymbol{M_G^{-1}} = \boldsymbol{K_G^T}\left(\boldsymbol{M_G^{-1}}\right)^T = \left(\boldsymbol{M_G^{-1}}\,\boldsymbol{K_G}\right)^T = \boldsymbol{A}^T \tag{3.4}$$

The modal decomposition of the equations (2.1) will be based on the right and left complex conjugated eigenvectors $\boldsymbol{R}^{(j)}$ and $\boldsymbol{L}^{(j)}$ of the $\boldsymbol{A}$-matrix, calculated from (3.2a) resp. (3.2b):

$$\left(\boldsymbol{A} + \lambda^{(j)}\boldsymbol{E}\right)\boldsymbol{R}^{(j)} = \boldsymbol{0} \qquad \text{resp.} \qquad \left(\boldsymbol{A}^T + \lambda^{(j)}\boldsymbol{E}\right)\boldsymbol{L}^{(j)} = \boldsymbol{0} \tag{3.5a,b}$$

According to the formulations (3.2a) and (3.2b) a relation between an arbitrary j^{th} right and left eigenvector can be derived:

$$\boldsymbol{L}^{(j)} = \boldsymbol{K_G}\,\boldsymbol{R}^{(j)} \tag{3.6}$$

The eigenvector pairs are collected in the right and the left modal matrices $\boldsymbol{R}$ resp. $\boldsymbol{L}$:

$$\boldsymbol{R} = \begin{bmatrix}\boldsymbol{R}^{(1)} & \overline{\boldsymbol{R}}^{(1)} & \cdots & \boldsymbol{R}^{(n)} & \overline{\boldsymbol{R}}^{(n)}\end{bmatrix} \quad \text{resp.} \quad \boldsymbol{L} = \begin{bmatrix}\boldsymbol{L}^{(1)} & \overline{\boldsymbol{L}}^{(1)} & \cdots & \boldsymbol{L}^{(n)} & \overline{\boldsymbol{L}}^{(n)}\end{bmatrix} \tag{3.6a,b}$$

The main diagonal components $\gamma_{(j)}$ in the orthogonality relation (3.7) between the right and left modal matrices

$$\boldsymbol{R}^T\boldsymbol{L} = \boldsymbol{R}^T\boldsymbol{K_G}\boldsymbol{R} = \begin{bmatrix}\gamma_1 & & & & \\ & \overline{\gamma}_1 & & & \\ & & \cdots & & \\ & & & \gamma_n & \\ & & & & \overline{\gamma}_n\end{bmatrix} \tag{3.7}$$

are used to normalize both modal matrices:

$$\boldsymbol{\Phi}^{\boldsymbol{R}}_{(j)} = \frac{\boldsymbol{R}^{(j)}}{\sqrt{\gamma_j}} \quad \rightarrow \quad \boldsymbol{\Phi}^{\boldsymbol{R}} = \begin{bmatrix}\boldsymbol{\Phi}^{\boldsymbol{R}}_{(1)} & \overline{\boldsymbol{\Phi}}^{\boldsymbol{R}}_{(1)} & \cdots & \boldsymbol{\Phi}^{\boldsymbol{R}}_{(n)} & \overline{\boldsymbol{\Phi}}^{\boldsymbol{R}}_{(n)}\end{bmatrix} \tag{3.8a}$$

$$\boldsymbol{\Phi}^{\boldsymbol{L}}_{(j)} = \frac{\boldsymbol{L}^{(j)}}{\sqrt{\gamma_j}} \quad \rightarrow \quad \boldsymbol{\Phi}^{\boldsymbol{L}} = \begin{bmatrix}\boldsymbol{\Phi}^{\boldsymbol{L}}_{(1)} & \overline{\boldsymbol{\Phi}}^{\boldsymbol{L}}_{(1)} & \cdots & \boldsymbol{\Phi}^{\boldsymbol{L}}_{(n)} & \overline{\boldsymbol{\Phi}}^{\boldsymbol{L}}_{(n)}\end{bmatrix} \tag{3.8b}$$

The normalization (3.8) leads to the relationships

$$(\boldsymbol{\Phi}^{\boldsymbol{L}})^T\,\boldsymbol{\Phi}^{\boldsymbol{R}} = \;(\boldsymbol{\Phi}^{\boldsymbol{R}})^T\,\boldsymbol{\Phi}^{\boldsymbol{L}} = \boldsymbol{E} \tag{3.9}$$

$$\boldsymbol{\Phi}^{\boldsymbol{R}} = \;\{(\boldsymbol{\Phi}^{\boldsymbol{L}})^T\}^{-1} \quad \leftrightarrow \quad (\boldsymbol{\Phi}^{\boldsymbol{R}})^T = (\boldsymbol{\Phi}^{\boldsymbol{L}})^{-1} \tag{3.10}$$

where $\boldsymbol{E}$ is a (2n x 2n) identity matrix.

In order to derive the diagonalization of the $\boldsymbol{A}^T$-matrix the eigenvalue problem (3.5b) is reformulated by use of the $\boldsymbol{\Phi}^{\boldsymbol{L}}$-matrix:

$$\boldsymbol{A}^T\boldsymbol{\Phi}^{\boldsymbol{L}} + \boldsymbol{\Phi}^{\boldsymbol{L}}\,\boldsymbol{\Lambda} = \boldsymbol{0} \quad \rightarrow \quad \boldsymbol{A}^T = \boldsymbol{\Phi}^{\boldsymbol{L}}\,(-\boldsymbol{\Lambda})(\boldsymbol{\Phi}^{\boldsymbol{L}})^{-1} \quad \leftrightarrow \quad -\boldsymbol{\Lambda} = (\boldsymbol{\Phi}^{\boldsymbol{L}})^{-1}\boldsymbol{A}^T\boldsymbol{\Phi}^{\boldsymbol{L}} \tag{3.11}$$

where

$\boldsymbol{\Lambda} = \{\lambda^{(j)}\}$ $\quad (j = 1,2,\dots,2n)$ $\quad$ is the spectral matrix of $\boldsymbol{A}$.

In analogy to Eq.(2.9) new complex coordinates $\boldsymbol{B^L}$ are introduced by

$$\boldsymbol{F} = \begin{bmatrix}\boldsymbol{D} & \boldsymbol{K}\\ \boldsymbol{K} & \end{bmatrix}\begin{bmatrix}\dot{\boldsymbol{V}}\\ \boldsymbol{V}\end{bmatrix} = \boldsymbol{\Phi}^{\boldsymbol{L}}\,\boldsymbol{B}^{\boldsymbol{L}}(t) = \;\boldsymbol{\Phi}^{\boldsymbol{L}}[a^{(1)}(t) \quad b^{(1)}(t) \quad \cdots \quad a^{(n)}(t) \quad b^{(n)}(t)]^T \tag{3.12}$$

Including the modal coordinates from (3.12) into (3.2b), the equations of motion are transformed into a set of 2n uncoupled complex equations:

$$\underbrace{(\boldsymbol{\Phi}^L)^{-1}\boldsymbol{E}\,\boldsymbol{\Phi}^L}_{\begin{bmatrix}1 & & \\ & \cdots & \\ & & 1\end{bmatrix}}\dot{\boldsymbol{B}}^L + \underbrace{(\boldsymbol{\Phi}^L)^{-1}\boldsymbol{K}_G\,\boldsymbol{M}_G^{-1}\boldsymbol{\Phi}^L}_{\begin{bmatrix}-\lambda^{(1)} & & & & \\ & -\bar{\lambda}^{(1)} & & & \\ & & \cdots & & \\ & & & -\lambda^{(n)} & \\ & & & & -\bar{\lambda}^{(n)}\end{bmatrix}}\boldsymbol{B}^L = \underbrace{(\boldsymbol{\Phi}^L)^{-1}\boldsymbol{A}^T\boldsymbol{P}}_{\begin{bmatrix}p_{a1}^L \\ p_{b1}^L \\ \cdots \\ p_{an}^L \\ p_{bn}^L\end{bmatrix}} \tag{3.13}$$

3.2 Alternative form of the equation of single mass oscillator

The form (2.11) of the general eigenvalue problem and his solution - Eq. (2.13), remain the same. The eigenvectors $\mathbf{r}_j$ $(j = 1{,}2)$ are **right eigenvectors** of the matrix $\boldsymbol{a} = \boldsymbol{m}^{-1}\boldsymbol{k}$. In order to determine the left eigenvectors of the matrix $\boldsymbol{a}$ we introduce the substitution

$$\underbrace{\begin{bmatrix}f_1 \\ f_2\end{bmatrix}}_{\boldsymbol{f}} = \underbrace{\begin{bmatrix}2\eta\omega & \omega^2 \\ \omega^2 & \end{bmatrix}}_{\boldsymbol{k}}\underbrace{\begin{bmatrix}\dot{v} \\ v\end{bmatrix}}_{\boldsymbol{q}}$$

$$\boldsymbol{f} = \boldsymbol{k}\boldsymbol{q} \tag{3.14}$$

An alternative form of the equation of motion is

$$\underbrace{\boldsymbol{k}\dot{\boldsymbol{q}}} + \boldsymbol{k}(\boldsymbol{m}^{-1}\boldsymbol{k})\boldsymbol{q} = \boldsymbol{k}\,\boldsymbol{m}^{-1}\boldsymbol{p}$$

$$\dot{\boldsymbol{f}} + \boldsymbol{k}\,\boldsymbol{m}^{-1}\boldsymbol{f} = \boldsymbol{k}\,\boldsymbol{m}^{-1}\boldsymbol{p}$$

$$\underbrace{\begin{bmatrix}1 & \\ & 1\end{bmatrix}}_{\boldsymbol{e}}\underbrace{\begin{bmatrix}\dot{f}_1 \\ \dot{f}_2\end{bmatrix}}_{\dot{\boldsymbol{f}}} + \underbrace{\begin{bmatrix}2\eta\omega & -1 \\ \omega^2 & \end{bmatrix}}_{\boldsymbol{k}\boldsymbol{m}^{-1}}\underbrace{\begin{bmatrix}f_1 \\ f_2\end{bmatrix}}_{\boldsymbol{f}} = \underbrace{\begin{bmatrix}2\eta\omega & -1 \\ \omega^2 & \end{bmatrix}}_{\boldsymbol{k}\boldsymbol{m}^{-1}}\underbrace{\begin{bmatrix}p(t) \\ \end{bmatrix}}_{\boldsymbol{p}} \tag{3.15}$$

The corresponding eigenvalue problem is

$$\left(\underbrace{\boldsymbol{k}\,\boldsymbol{m}^{-1}}_{\boldsymbol{a}^T} + \lambda^{(j)}\boldsymbol{e}\right)\boldsymbol{l} = \boldsymbol{0}\,. \tag{3.16}$$

The $\boldsymbol{a}^T$-matrix in (3.16) is formulated due to the symmetry of $\boldsymbol{k}$ and $\boldsymbol{m}$:

$$\boldsymbol{a}^T = (\boldsymbol{m}^{-1}\boldsymbol{k})^T = \boldsymbol{k}^T\,(\boldsymbol{m}^{-1})^T = \boldsymbol{k}\,\boldsymbol{m}^{-1} \tag{3.17}$$

The two eigenvalues λ, $\bar{\lambda}$ of (3.16) remain the same - Eq. (2.14), but the corresponding complex conjugate eigenvectors are now

$$\left.\begin{matrix}\boldsymbol{l}_1 \\ \boldsymbol{l}_2\end{matrix}\right\} = \boldsymbol{l}_r \pm i\boldsymbol{l}_i = \begin{bmatrix}\frac{\eta \mp i\sqrt{1-\eta^2}}{\omega} \\ 1\end{bmatrix} \tag{3.18}$$

Rewriting the eigenvalue problem (3.16) to

$$\boldsymbol{l}_j^{\,T}\left(\boldsymbol{a} + \lambda^{(j)}\boldsymbol{e}\right) = \boldsymbol{0}^T \quad \rightarrow \quad \left(\boldsymbol{a}^T + \lambda^{(j)}\boldsymbol{e}\right)\boldsymbol{l}_j = \boldsymbol{0}\ , \tag{3.19}$$

we recognize that $\boldsymbol{l}_j$ represents the **left eigenvectors** of the matrix $\boldsymbol{a} = \boldsymbol{m}^{-1}\boldsymbol{k}$ (respectively, the right eigenvectors of the matrix $\boldsymbol{a}^T = \boldsymbol{k}\,\boldsymbol{m}^{-1}$).

In this variant the modal matrix is defined without normalization by

$$\boldsymbol{\varphi}^{\mathbf{L}} = [\boldsymbol{l}_1 \quad \boldsymbol{l}_2] = \begin{bmatrix}\frac{\eta - i\sqrt{1-\eta^2}}{\omega} & \frac{\eta + i\sqrt{1-\eta^2}}{\omega} \\ 1 & 1\end{bmatrix} \tag{3.20}$$

Rewriting the eigenvalue problem in the „left" formulation (3.19) using the $\boldsymbol{\varphi^L}$ modal matrix

$$\boldsymbol{a^T \varphi^L} + \boldsymbol{\varphi^L \lambda} = \mathbf{0} \qquad \leftarrow \quad \boldsymbol{\lambda} = \begin{bmatrix} \lambda & \\ & \bar{\lambda} \end{bmatrix} \tag{3.21}$$

The diagonalization of the matrix $\boldsymbol{a^T}$ and the inverse relation can be developed to

$$\boldsymbol{a^T} = \boldsymbol{\varphi^L}(-\boldsymbol{\lambda})\,(\boldsymbol{\varphi^L})^{-1} \qquad \leftrightarrow \qquad -\boldsymbol{\lambda} = (\boldsymbol{\varphi^L})^{-1}\boldsymbol{a^T}\,\boldsymbol{\varphi^L} \tag{3.22}$$

where

$$(\boldsymbol{\varphi^L})^{-1} = \frac{1}{2\sqrt{1-\eta^2}}\begin{bmatrix} i\omega & \sqrt{1-\eta^2} - i\eta \\ -i\omega & \sqrt{1-\eta^2} + i\eta \end{bmatrix} \tag{3.23}$$

3.3 Transformation of the MDOFS equations in real space

We introduce into the uncoupled complex modal equations (3.13) new real coordinates $[x^{(j)} \quad y^{(j)}]^T$ for each j-th eigenpair, defined by

$$\begin{bmatrix} a^{(j)}(t) \\ b^{(j)}(t) \end{bmatrix} = \left(\boldsymbol{\varphi^{L(j)}}\right)^{-1} \begin{bmatrix} x^{(j)}(t) \\ y^{(j)}(t) \end{bmatrix}^{\boldsymbol{L}} \tag{3.24}$$

With (3.24) the modal equations (3.13) can be transformed **in pairs** into the real form of SDOFS-equation (index (j) omitted), with regard to (3.22):

$$\begin{matrix} \underbrace{\boldsymbol{\varphi^L}\begin{bmatrix} 1 & \\ & 1 \end{bmatrix}(\boldsymbol{\varphi^L})^{-1}} & \cdot \begin{bmatrix} \dot{x} \\ \dot{y} \end{bmatrix}^{\boldsymbol{L}} & + & \underbrace{\boldsymbol{\varphi^L}\begin{bmatrix} -\lambda & \\ & -\bar{\lambda} \end{bmatrix}(\boldsymbol{\varphi^L})^{-1}} & \cdot \begin{bmatrix} x \\ y \end{bmatrix}^{\boldsymbol{L}} & = & \underbrace{\boldsymbol{\varphi^L}\begin{bmatrix} p_a^L \\ p_b^L \end{bmatrix}} \\ \begin{bmatrix} 1 & \\ & 1 \end{bmatrix} & \cdot \begin{bmatrix} \dot{x} \\ \dot{y} \end{bmatrix}^{\boldsymbol{L}} & + & \begin{bmatrix} 2\eta\omega & -1 \\ \omega^2 & \end{bmatrix} & \cdot \begin{bmatrix} x \\ y \end{bmatrix}^{\boldsymbol{L}} & = & \begin{bmatrix} g^L(t) \\ h^L(t) \end{bmatrix} \end{matrix} \tag{3.25}$$

A purely real (2n x 2n) transformation basis $\boldsymbol{Y^L}$ can be built up by combination of the two complex transformations (3.12) and (3.24):

$$\boldsymbol{F} = \begin{bmatrix} \boldsymbol{D} & \boldsymbol{K} \\ \boldsymbol{K} & \end{bmatrix}\begin{bmatrix} \dot{\boldsymbol{V}} \\ \boldsymbol{V} \end{bmatrix} = \boldsymbol{\Phi^L} \underbrace{\begin{bmatrix} \left(\boldsymbol{\varphi^{L(1)}}\right)^{-1} & & \\ & \cdots & \\ & & \left(\boldsymbol{\varphi^{L(n)}}\right)^{-1} \end{bmatrix}}_{(\Psi_L)^{-1}} \begin{bmatrix} x_1 \\ y_1 \\ \cdots \\ x_n \\ y_n \end{bmatrix}^{\boldsymbol{L}} = \underbrace{\boldsymbol{\Phi^L}\,(\Psi_L)^{-1}}_{\boldsymbol{Y_L}}\mathbf{X}^{\boldsymbol{L}} = \boldsymbol{Y_L}\,\mathbf{X}^{\boldsymbol{L}} \tag{3.26a}$$

With regard to Eq. (3.10) the inverse of the transformation basis $\boldsymbol{Y_L}$ can be written to

$$\boldsymbol{Y_L}^{-1} = \Psi_L \cdot (\boldsymbol{\Phi^L})^{-1} = \underbrace{\begin{bmatrix} \left(\boldsymbol{\varphi^{L(1)}}\right) & & \\ & \cdots & \\ & & \left(\boldsymbol{\varphi^{L(n)}}\right) \end{bmatrix}}_{\Psi_L} \cdot (\boldsymbol{\Phi^R})^T \tag{3.26b}$$

Finally the equations of motion (3.2b) can be uncoupled by means of the transformation basis $\boldsymbol{Y_L}$ and the inverse matrix $\boldsymbol{Y_L}^{-1}$ into n real-space SDOFS block equations from type of (3.25):

$$\underbrace{{\boldsymbol{Y_L}}^{-1}\cdot\boldsymbol{E}\cdot\boldsymbol{Y_L}}_{\begin{bmatrix}1&&&\\&1&&\\&&\cdots&\\&&&1\end{bmatrix}}\cdot\underbrace{\begin{bmatrix}\dot{x}^{(1)}\\\dot{y}^{(1)}\\\cdots\\\dot{x}^{(n)}\\\dot{y}^{(n)}\end{bmatrix}^{\boldsymbol{L}}}_{\dot{\boldsymbol{X}}^{\boldsymbol{L}}}+\underbrace{{\boldsymbol{Y_L}}^{-1}\cdot\overbrace{\left(\boldsymbol{K_G}\,\boldsymbol{M_G^{-1}}\right)}^{\boldsymbol{A^T}}\cdot\boldsymbol{Y_L}}_{\begin{bmatrix}2\eta_1\,\omega_1&-1&&&\\\omega_1^2&0&&&\\&&\cdots&&\\&&&2\eta_n\,\omega_n&-1\\&&&\omega_n^2&0\end{bmatrix}}\cdot\underbrace{\begin{bmatrix}x^{(1)}\\y^{(1)}\\\cdots\\x^{(n)}\\y^{(n)}\end{bmatrix}^{\boldsymbol{L}}}_{\boldsymbol{X}^{\boldsymbol{L}}}=\underbrace{{\boldsymbol{Y_L}}^{-1}\cdot\boldsymbol{A^T}\left[\boldsymbol{p}\right]}_{\begin{bmatrix}g_1\\h_1\\\cdots\\g_n\\h_n\end{bmatrix}^{\boldsymbol{L}}} \tag{3.27}$$

The solution of each j[th] SDOFS block equation in (3.27) is performed eliminating first the modal coordinate $x(t)$ (index (j) omitted):

$$\begin{bmatrix}1&\\&1\end{bmatrix}\begin{bmatrix}\dot{x}\\\dot{y}\end{bmatrix}^{\boldsymbol{L}}+\begin{bmatrix}2\eta\omega&-1\\\omega^2&\end{bmatrix}\begin{bmatrix}x\\y\end{bmatrix}^{\boldsymbol{L}}=\begin{bmatrix}g_L(t)\\h_L(t)\end{bmatrix} \tag{3.28}$$

Introducing the second equation

$$x=-\frac{\dot{y}}{\omega^2}+\frac{h_L}{\omega^2} \tag{3.29a}$$

into the first one to receive

$$\ddot{y}+2\eta\omega\,\dot{y}+\omega^2\,y=-\omega^2\,g_L+2\eta\omega\,h_L+\dot{h}_L \tag{3.29b}$$

The modal response $y(t)$ is easy determined by step-by-step integration of Eq. (3.29b), $x(t)$ should be calculated according to (3.29a). The final time response of the original n DOFs is calculated by superposition of the modal coordinates in accordance to Eq. (3.26) and (3.1):

$$\begin{bmatrix}\dot{\boldsymbol{V}}\\\boldsymbol{V}\end{bmatrix}=(\mathbf{K}_{\boldsymbol{G}})^{-1}\,\boldsymbol{Y_L}\,\mathbf{X}^{\boldsymbol{L}} \tag{3.30}$$

3.4 Analytical form of the real modal transformation

The components of the real space matrix $\boldsymbol{Y_L}$, which belong to the j[th] eigenvector-pair, are the following two columns - see (3.23), (3.26), (index (j) omitted):

$$\begin{aligned}\left[\cdots\quad(\boldsymbol{Y}_x)^{(j)}\quad\left(\boldsymbol{Y}_y\right)^{(j)}\quad\cdots\right]&=\left[\boldsymbol{\Phi}_r^{\boldsymbol{L}}+i\boldsymbol{\Phi}_i^{\boldsymbol{L}}\quad\boldsymbol{\Phi}_r^{\boldsymbol{L}}-i\boldsymbol{\Phi}_i^{\boldsymbol{L}}\right]\cdot\frac{1}{2\sqrt{1-\eta^2}}\begin{bmatrix}i\omega&\sqrt{1-\eta^2}-i\eta\\-i\omega&\sqrt{1-\eta^2}+i\eta\end{bmatrix}\\&=\frac{1}{\sqrt{1-\eta^2}}\left[\cdots\quad-\omega\,\boldsymbol{\Phi}_i^{\boldsymbol{L}}\quad\left(\boldsymbol{\Phi}_r^{\boldsymbol{L}}\sqrt{1-\eta^2}+\boldsymbol{\Phi}_i^{\boldsymbol{L}}\,\eta\right)\quad\cdots\right]\end{aligned} \tag{3.31}$$

The associated two components of the “right side” vector in (3.27) are - with regard to (3.26) and (3.10) - fully real too:

$$\begin{bmatrix}\cdots\\g_L\\h_L\\\cdots\end{bmatrix}=(\boldsymbol{Y_L})^{-1}\boldsymbol{A}^T\boldsymbol{P}=\boldsymbol{\Psi}_{\mathrm{L}}\underbrace{(\boldsymbol{\Phi}^{\boldsymbol{L}})^{-1}}_{(\boldsymbol{\Phi}^{\boldsymbol{R}})^{\mathrm{T}}}\boldsymbol{A}^T\boldsymbol{P}=\begin{bmatrix}\cdots\\\frac{2}{\omega}\left(\eta\,(\boldsymbol{\Phi}_r^{\boldsymbol{R}})^{\mathrm{T}}+\sqrt{1-\eta^2}\left(\boldsymbol{\Phi}_i^{\boldsymbol{R}}\right)^{\mathrm{T}}\right)\\2(\boldsymbol{\Phi}_r^{\boldsymbol{R}})^{\mathrm{T}}\\\cdots\end{bmatrix}\boldsymbol{A}^T\boldsymbol{P} \tag{3.32}$$

4 NUMERICAL EXAMPLE

4.1 Structural data, geometry and loads

The numerical example considers the vibrations of a small rotor blade subjected to wind thrust load, it has been first presented in (E. Stanoev, 2017). The equations of motion in the form (3.2) are solved applying the proposed modal decomposition method in Section 3 employing only the first four lowest natural frequencies and the associated four eigenmodes. Considered are two cases: non-proportional and proportional damping.

The finite element solution is based on the numerical integration of the system of differential equations for the Bernoulli-beam. The reference axis of the beam model coincides with the centre of the circular-section at the root. Thereby the differential equations and all cross section stiffness data are referred to the real rotational axis of the rotor blade, accounting for the eccentric mass application.

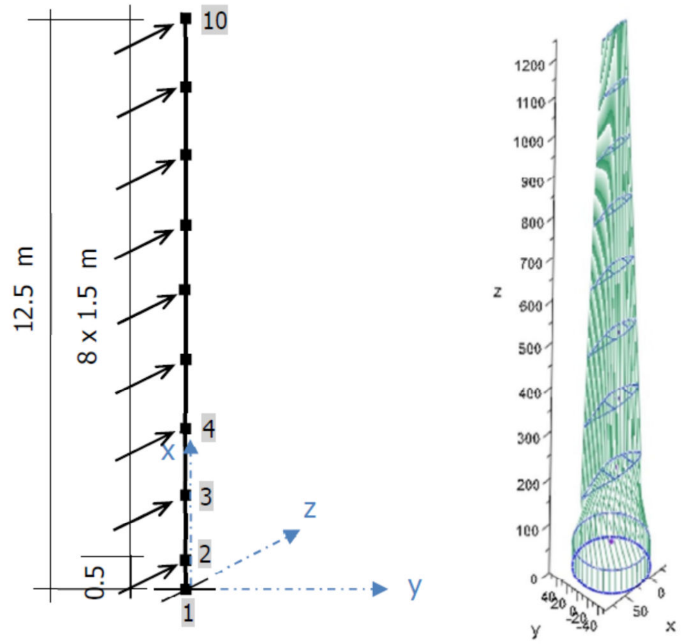

Fig. 1 - Rotor blade beam model subjected to wind loads

The stiffness data of the blade thin-wall cross sections have been calculated in (Nan Li, 2015). The generic aerodynamic blade geometry has been derived from real blade data.

The wind loads are calculated according to the formula for the aerodynamic lift force per unit length of an aerofoil, see (T. Burton, 2011), p. 59:

$$L = \frac{1}{2}\rho \cdot c(r) \cdot W^2 \cdot C_L \tag{4.1}$$

where: W : air velocity relative to the aerofoil

ρ : air density = 1.225 [kg/m^3]

$c(r)$: chord of the aerofoil

C_L : lift coefficient $C_L = 2\pi\,\alpha = 2\pi\left(\frac{\pi}{180}6.0\right) = 0.658$,

the flow angle α is assumed to be 6.0 [deg]

The air velocity W is the vector sum of the rotational speed Ω (assumed to reach 60 rpm in the initial four seconds) and the wind speed u, incident on the aerofoil in accordance with the Betz-theory (T. Burton, 2011):

$$W = \sqrt{(\Omega\, r)^2 + \left(\frac{2}{3}u\right)^2} \qquad \text{where } \Omega = \left(\frac{60}{30}\pi\right) \text{ in [rad/s]} \tag{4.2}$$

Time series of a real wind speed measurements $u(t)$ are used to calculate the wind thrust force, shown in Figure 2:

Fig. 2 - Wind thrust function acting on the rotor blade at 12.5 m

The resulting wind thrust loads $\mathrm{T}(t)$ per unit length along the x-axis of the rotor blade can be determined as function of the wind speed $u(t)$. In the structural model the wind thrust loads are acting as summarized nodal forces - see fig. 1.

4.2 The damping approach

In order to determine the proportional damping matrix $\boldsymbol{D_p}$, see the equations of motion (2.1), the lowest four natural frequencies and associated periods for the undamped system are calculated to be

$$\begin{aligned} f_1 &= 2.643\ [s^{-1}] & T_1 &= 0.378\ [s] \\ f_2 &= 4.622\ [s^{-1}] & T_2 &= 0.216\ [s] \\ f_3 &= 7.942\ [s^{-1}] & T_3 &= 0.126\ [s] \\ f_4 &= 16.650\ [s^{-1}] & T_4 &= 0.060\ [s] \end{aligned} \tag{4.3}$$

Stiffness proportional damping as a special case of Rayleigh damping has been assumed:

$$\boldsymbol{D_p} = \beta\, \boldsymbol{K} \qquad \text{where} \qquad \beta = \frac{2\eta}{\omega_1} = \frac{\eta\, T_1}{\pi} = 0.000964[s] \tag{4.4}$$

In Eq. (4.4) the damping ratio $\eta = 0.008$ for the first natural period T_1 has been taken in accordance with [21] p. 249.

The non-proportional symmetric damping matrix $\boldsymbol{D_{np}}$, including structural (proportional) and aerodynamic damping is build by

$$\boldsymbol{D_{np}} = \boldsymbol{D_p} + \boldsymbol{D_a} \tag{4.5}$$

where the matrix $\boldsymbol{D_a}$ represents aerodynamic damping. The formulation is based on a simple expression for the aerodynamic damping coefficient $c_d(r)$ per unit length, given in (T. Burton, 2011), p. 247:

$$c_d(r) = \frac{1}{2}\rho \cdot \Omega r \cdot c(r) \cdot \frac{dC_L}{d\alpha} \quad \left[\frac{kg}{s}\,\frac{1}{m}\right], \quad \text{where} \quad \frac{dC_L}{d\alpha} = 2\pi \tag{4.6}$$

The associate symmetric damping matrix $\boldsymbol{D_a}$ for the Bernoulli-beam element is derived by analogy with the method presented in (E. Stanoev, 2007) for the finite-element mass matrix, for more details see (E. Stanoev, 2017).

4.3 Non-proportionally damped system

System damping matrix here is $\boldsymbol{D_{np}}$ - Eq. (4.5). The vector of the first ten complex conjugate eigenvalue pairs of the matrix $\boldsymbol{A} = \boldsymbol{M_G^{-1}}\,\boldsymbol{K_G}$, see Eq. (3.5), is

$$\begin{pmatrix} -5.56181 + 15.7652\,i \\ -5.56181 - 15.7652\,i \\ -0.40981 + 29.0336\,i \\ -0.40981 - 29.0336\,i \\ -6.33469 + 49.2454\,i \\ -6.33469 - 49.2454\,i \\ -9.53814 + 104.542\,i \\ -9.53814 - 104.542\,i \\ -5.43041 + 105.219\,i \\ -5.43041 - 105.219\,i \\ -20.7608 + 185.185\,i \\ -20.7608 - 185.185\,i \\ -22.1068 + 207.402\,i \\ -22.1068 - 207.402\,i \\ -27.8796 + 238.91\,i \\ -27.8796 - 238.91\,i \\ -45.8047 + 292.379\,i \\ -45.8047 - 292.379\,i \\ -63.5216 + 353.962\,i \\ -63.5216 - 353.962\,i \end{pmatrix} \tag{4.7}$$

The number of modes considered in the modal transformation is limited to the first four eigenvector pairs. The structural system in Figure 1 has 54 DOF. The corresponding (108x8) normalized modal matrix $\boldsymbol{\Phi^L}$ - Eq. (3.8b), is computed to (only the first ten rows are printed)

$$\begin{pmatrix}
1.37\,10^{-5}-6.42\,10^{-6}\,i & 1.37\,10^{-5}+6.42\,10^{-6}\,i & -2.82\,10^{-5}+2.77\,10^{-5}\,i & -2.82\,10^{-5}-2.77\,10^{-5}\,i & -1.64\,10^{-5}-2.16\,10^{-5}\,i & -1.64\,10^{-5}+2.16\,10^{-5}\,i & 4.3\,10^{-5}-1.94\,10^{-5}\,i & 4.3\,10^{-5}+1.94\,10^{-5}\,i \\
-5.71\,10^{-6}-5.97\,10^{-7}\,i & -5.71\,10^{-6}+5.97\,10^{-7}\,i & 2.86\,10^{-4}-2.78\,10^{-4}\,i & 2.86\,10^{-4}+2.78\,10^{-4}\,i & -1.22\,10^{-6}+3.13\,10^{-6}\,i & -1.22\,10^{-6}-3.13\,10^{-6}\,i & -1.02\,10^{-4}-1.0\,10^{-4}\,i & -1.02\,10^{-4}+1.0\,10^{-4}\,i \\
5.06\,10^{-4}-2.47\,10^{-4}\,i & 5.06\,10^{-4}+2.47\,10^{-4}\,i & 1.27\,10^{-5}-1.12\,10^{-6}\,i & 1.27\,10^{-5}+1.12\,10^{-6}\,i & -6.6\,10^{-4}-8.56\,10^{-4}\,i & -6.6\,10^{-4}+8.56\,10^{-4}\,i & 0.00143-0.00116\,i & 0.00143+0.00116\,i \\
8.73\,10^{-5}-3.98\,10^{-5}\,i & 8.73\,10^{-5}+3.98\,10^{-5}\,i & 8.45\,10^{-6}-6.19\,10^{-6}\,i & 8.45\,10^{-6}+6.19\,10^{-6}\,i & -1.19\,10^{-4}-1.56\,10^{-4}\,i & -1.19\,10^{-4}+1.56\,10^{-4}\,i & 2.85\,10^{-4}-2.32\,10^{-4}\,i & 2.85\,10^{-4}+2.32\,10^{-4}\,i \\
-1.85\,10^{-4}+9.04\,10^{-5}\,i & -1.85\,10^{-4}-9.04\,10^{-5}\,i & -4.36\,10^{-6}+1.7\,10^{-7}\,i & -4.36\,10^{-6}-1.7\,10^{-7}\,i & 2.39\,10^{-4}+3.09\,10^{-4}\,i & 2.39\,10^{-4}-3.09\,10^{-4}\,i & -5.1\,10^{-4}+4.16\,10^{-4}\,i & -5.1\,10^{-4}-4.16\,10^{-4}\,i \\
-3.02\,10^{-6}+1.27\,10^{-7}\,i & -3.02\,10^{-6}-1.27\,10^{-7}\,i & 1.13\,10^{-4}-1.1\,10^{-4}\,i & 1.13\,10^{-4}+1.1\,10^{-4}\,i & 5.53\,10^{-7}+2.57\,10^{-6}\,i & 5.53\,10^{-7}-2.57\,10^{-6}\,i & -4.16\,10^{-5}-3.66\,10^{-5}\,i & -4.16\,10^{-5}+3.66\,10^{-5}\,i \\
5.02\,10^{-5}-2.36\,10^{-5}\,i & 5.02\,10^{-5}+2.36\,10^{-5}\,i & -1.38\,10^{-4}+1.36\,10^{-4}\,i & -1.38\,10^{-4}-1.36\,10^{-4}\,i & -5.52\,10^{-5}-7.21\,10^{-5}\,i & -5.52\,10^{-5}+7.21\,10^{-5}\,i & 1.41\,10^{-4}-4.93\,10^{-5}\,i & 1.41\,10^{-4}+4.93\,10^{-5}\,i \\
-1.86\,10^{-4}+2.73\,10^{-5}\,i & -1.86\,10^{-4}-2.73\,10^{-5}\,i & 0.00512-0.00498\,i & 0.00512+0.00498\,i & 8.16\,10^{-5}+1.86\,10^{-4}\,i & 8.16\,10^{-5}-1.86\,10^{-4}\,i & -0.00184-0.00138\,i & -0.00184+0.00138\,i \\
0.00721-0.00361\,i & 0.00721+0.00361\,i & 1.52\,10^{-4}+7.65\,10^{-6}\,i & 1.52\,10^{-4}-7.65\,10^{-6}\,i & -0.00881-0.0113\,i & -0.00881+0.0113\,i & 0.0171-0.0141\,i & 0.0171+0.0141\,i \\
8.69\,10^{-4}-4.22\,10^{-4}\,i & 8.69\,10^{-4}+4.22\,10^{-4}\,i & 7.08\,10^{-5}-4.97\,10^{-5}\,i & 7.08\,10^{-5}+4.97\,10^{-5}\,i & -0.00108-0.0014\,i & -0.00108+0.0014\,i & 0.00222-0.00184\,i & 0.00222+0.00184\,i
\end{pmatrix} \tag{4.8}$$

The matrix $(\boldsymbol{\Psi}_{\mathrm{L}})^{-1}$ is calculated in the case of four involved eigenmodes according to Eq. (3.26a), (3.23):

$$(\boldsymbol{\Psi}_{\mathrm{L}})^{-1} = \begin{bmatrix} (\boldsymbol{\varphi}^{L(1)})^{-1} & & & \\ & (\boldsymbol{\varphi}^{L(2)})^{-1} & & \\ & & (\boldsymbol{\varphi}^{L(3)})^{-1} & \\ & & & (\boldsymbol{\varphi}^{L(4)})^{-1} \end{bmatrix} =$$

$$\begin{pmatrix} 8.86368\,i & 0.5-0.176395\,i & 0 & 0 & 0 & 0 & 0 & 0 \\ -8.86368\,i & 0.5+0.176395\,i & 0 & 0 & 0 & 0 & 0 & 0 \\ 0 & 0 & 14.5197\,i & 0.5-0.00705752\,i & 0 & 0 & 0 & 0 \\ 0 & 0 & -14.5197\,i & 0.5+0.00705752\,i & 0 & 0 & 0 & 0 \\ 0 & 0 & 0 & 0 & 25.0301\,i & 0.5-0.0643176\,i & 0 & 0 \\ 0 & 0 & 0 & 0 & -25.0301\,i & 0.5+0.0643176\,i & 0 & 0 \\ 0 & 0 & 0 & 0 & 0 & 0 & 52.7059\,i & 0.5-0.0456189\,i \\ 0 & 0 & 0 & 0 & 0 & 0 & -52.7059\,i & 0.5+0.0456189\,i \end{pmatrix} \tag{4.9}$$

Finally the (108x8) real transformation matrix $\boldsymbol{Y_L}$ is computed according to (3.26a) - here only the first ten rows:

$$\mathbf{Y} = \begin{pmatrix} 0.000114 & 0.000011 & -0.000805 & -0.000028 & 0.00108 & -0.000019 & 0.002046 & 0.000041 \\ 0.000011 & -0.000006 & 0.008082 & 0.000282 & -0.000157 & -0.000001 & 0.010542 & -0.000111 \\ 0.004376 & 0.000419 & 0.000033 & 0.000013 & 0.042861 & -0.00077 & 0.122636 & 0.001321 \\ 0.000705 & 0.000073 & 0.00018 & 0.000008 & 0.007831 & -0.000139 & 0.024502 & 0.000264 \\ -0.001603 & -0.000153 & -0.000005 & -0.000004 & -0.015486 & 0.000279 & -0.043862 & -0.000472 \\ -0.000002 & -0.000003 & 0.003181 & 0.000111 & -0.000129 & 0.000001 & 0.00386 & -0.000045 \\ 0.000419 & 0.000042 & -0.003937 & -0.000136 & 0.003607 & -0.000065 & 0.005194 & 0.000136 \\ -0.000485 & -0.000176 & 0.144563 & 0.005047 & -0.009325 & 0.000106 & 0.14576 & -0.001968 \\ 0.063952 & 0.005941 & -0.000222 & 0.000152 & 0.563338 & -0.010255 & 1.481246 & 0.015774 \\ 0.007486 & 0.00072 & 0.001443 & 0.00007 & 0.069849 & -0.001264 & 0.193857 & 0.002051 \end{pmatrix} \tag{4.10}$$

After the modal transformation the time-dependent "load" vector is calculated to be a function of the wind thrust time series, see Figure 2:

$$\begin{bmatrix} g_1(t) \\ h_1(t) \\ \cdots \\ g_4(t) \\ h_4(t) \end{bmatrix}^{L} = \boldsymbol{Y_L}^{-1} \cdot \boldsymbol{A}^{T} \left[\boldsymbol{p}\right] = \begin{pmatrix} -0.572146\,u^2 \\ 2506.4\,u^2 \\ -1.45159\,u^2 \\ 150.11\,u^2 \\ -79.8106\,u^2 \\ -1187.78\,u^2 \\ -24.9309\,u^2 \\ 4973.28\,u^2 \end{pmatrix} \tag{4.11}$$

Four uncoupled SDOFS block equations from type of Eq. (3.25) are solved by step-by-step integration according to (3.29a-b):

$$\begin{bmatrix} 1 & & & & & \\ & -\omega_1^2 & & & & \\ & & \cdots & & & \\ & & & 1 & & \\ & & & & -\omega_n^2 \end{bmatrix} \cdot \underbrace{\begin{bmatrix} \dot{x}_1 \\ \dot{y}_1 \\ \cdots \\ \dot{x}_n \\ \dot{y}_n \end{bmatrix}}_{\dot{\mathbf{x}}} + \begin{bmatrix} 2\eta_1\,\omega_1 & \omega_1^2 & & & \\ \omega_1^2 & 0 & & & \\ & & \cdots & & \\ & & & 2\eta_n\,\omega_n & \omega_n^2 \\ & & & \omega_n^2 & 0 \end{bmatrix} \cdot \underbrace{\begin{bmatrix} x_1 \\ y_1 \\ \cdots \\ x_n \\ y_n \end{bmatrix}}_{\mathbf{x}} = \begin{bmatrix} g_1 \\ h_1 \\ \cdots \\ g_n \\ h_n \end{bmatrix}, \qquad (n = 4)$$

(4.12)

where $[\omega_i] =$ (16.7175 29.0365 49.6511 104.976)

$[\eta_i] =$ (0.332693 0.0141136 0.127584 0.0908603) (4.13a,b)

The vibration-response in the next figures has been determined in the time 0… 25.6 s, the time step length for the applied Newmark integration method is 0.03665 s.

The time response of the modal coordinates $y_j(t), x_j(t)$, $(j = 1,2,3)$ are shown in Figures 3a-c:

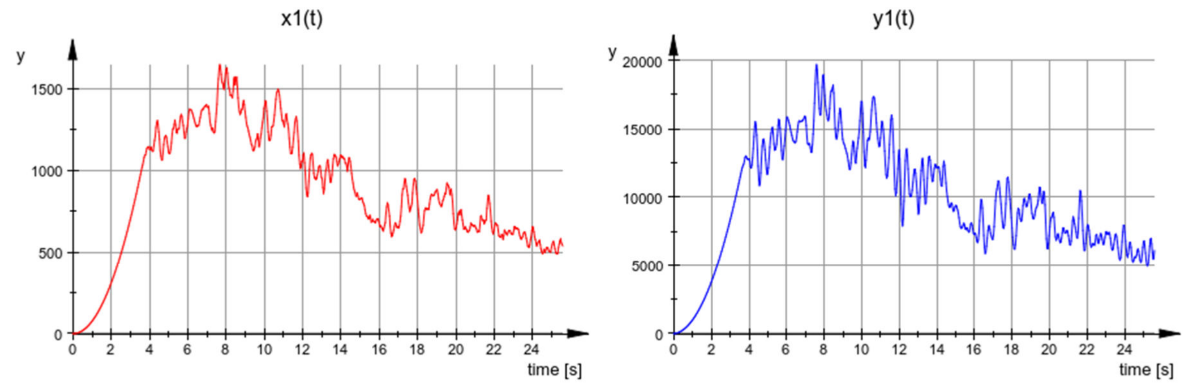

Fig. 3a - Time response of the modal coordinates $y_2(t), x_2(t)$ for the case "non-proportional damping"

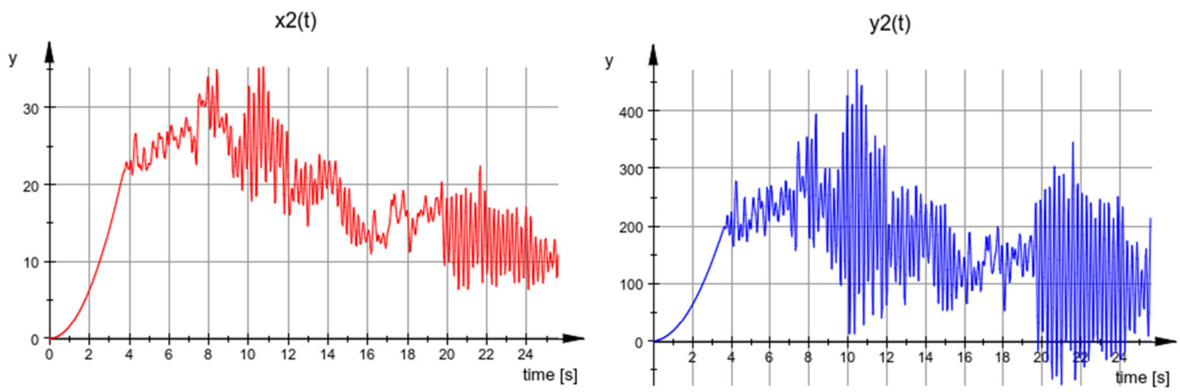

Fig. 3b - Time response of the modal coordinates $y_2(t), x_2(t)$ for the case "non-proportional damping"

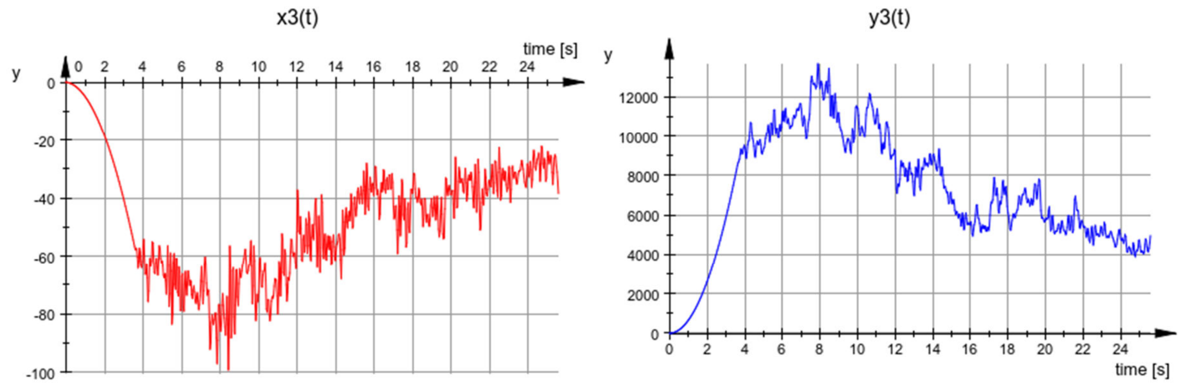

Fig. 3c - Time response of the modal coordinates $y_3(t), x_3(t)$ for the case "non-proportional damping"

The total responses for the original state variables $\boldsymbol{V}(t)$, $\dot{\boldsymbol{V}}(t)$, obtained by a back transformation according to Eq. (3.30), are plotted in Figures 4-6 for the rotor blade tip:

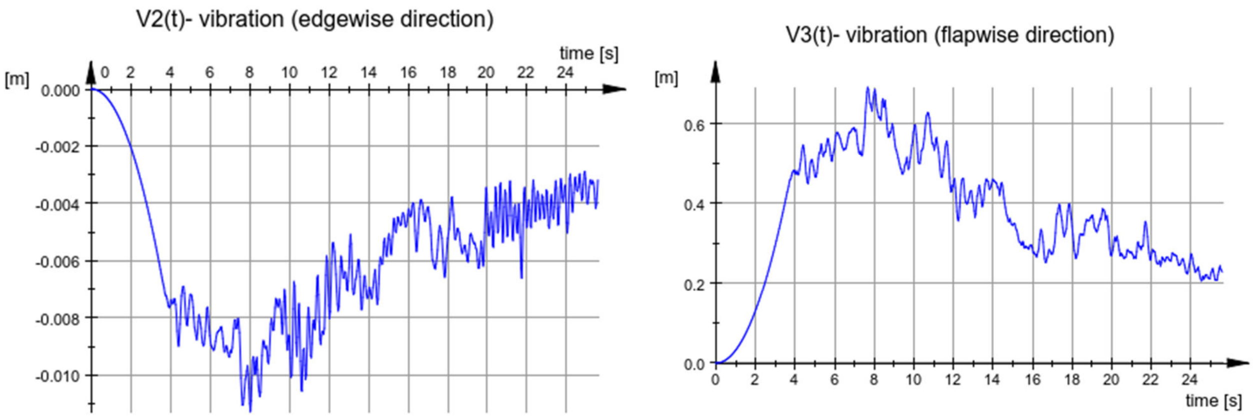

Fig. 4 - Total vibrations $u_2(t), u_3(t)$ $[m]$ (in y- and z-direction, see Fig.1) at the rotor blade tip - node #10

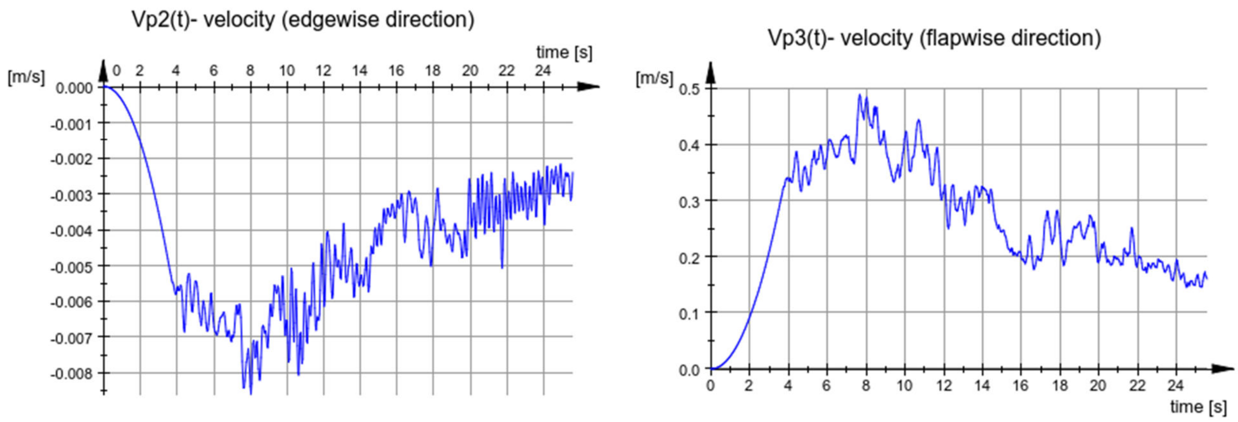

Fig. 5 - Velocities $\dot{u}_2(t), \dot{u}_3(t)$ $[m/s]$ (in y- and z-direction, see fig.1) at the rotor blade tip - node #10

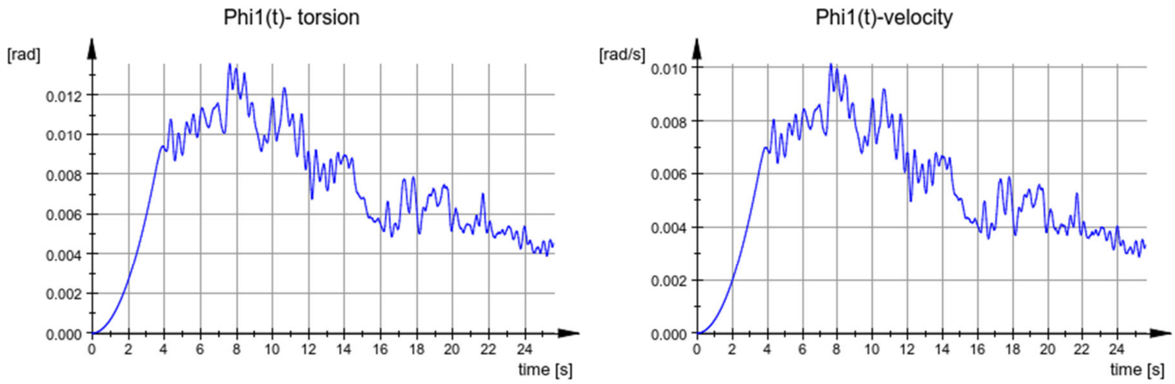

Fig. 6 - Torsional rotation resp. velocity $\varphi_1(t),\ \dot{\varphi}_1(t)$ at the rotor blade tip (node #10)

Comparison to the vibrations computed by direct step-by-step integration of the equations (2.1) shows no significant deviancies except for the torsional rotation. This is probably due to the absence of torsional eigenmode in the employed four eigenmodes.

4.4 Proportionally damped system

By using the symmetric damping matrix $\boldsymbol{D_p}$ - Eq. (4.4), the resulting ten lowest complex conjugate eigenvalue pairs are:

$$\begin{pmatrix} -0.132832+16.6035\,i \\ -0.132832-16.6035\,i \\ -0.406268+29.0352\,i \\ -0.406268-29.0352\,i \\ -1.19966+49.8844\,i \\ -1.19966-49.8844\,i \\ -5.27314+104.483\,i \\ -5.27314-104.483\,i \\ -5.39463+105.676\,i \\ -5.39463-105.676\,i \\ -16.7361+185.622\,i \\ -16.7361-185.622\,i \\ -20.9751+207.591\,i \\ -20.9751-207.591\,i \\ -27.8753+238.91\,i \\ -27.8753-238.91\,i \\ -42.2056+292.945\,i \\ -42.2056-292.945\,i \\ -62.3277+354.226\,i \\ -62.3277-354.226\,i \end{pmatrix} \tag{4.14}$$

The natural frequencies and the modal damping ratios associated to the four employed eigenmodes are in this case:

$$[\boldsymbol{\omega_i}] = (\,16.604\ \ 29.0381\ \ 49.8988\ \ 104.616\,)$$

$$[\eta_i] = (\,0.008\ \ 0.0139909\ \ 0.0240418\ \ 0.0504049\,) \tag{4.15a-b}$$

The (108x8) real transformation matrix Y_L, computed in regard with Eq. (3.26a), has now the form (only the first ten rows are printed):

$$\boldsymbol{Y_L} = \begin{pmatrix} 0.000175 & 0.000011 & -0.000799 & -0.000028 & 0.000978 & -0.000019 & 0.005827 & 0.000059 \\ -0.000077 & -0.000005 & 0.008081 & 0.000282 & -0.000069 & 0.000001 & -0.041588 & -0.000419 \\ 0.006449 & 0.000392 & 0.000262 & 0.000009 & 0.038976 & -0.000763 & 0.092832 & 0.000936 \\ 0.001104 & 0.000067 & 0.000221 & 0.000008 & 0.007073 & -0.000138 & 0.017494 & 0.000176 \\ -0.002353 & -0.000143 & -0.000088 & -0.000003 & -0.014092 & 0.000276 & -0.033232 & -0.000335 \\ -0.00004 & -0.000002 & 0.003181 & 0.000111 & -0.000088 & 0.000002 & -0.016203 & -0.000163 \\ 0.000644 & 0.000039 & -0.003916 & -0.000137 & 0.003273 & -0.000064 & 0.021992 & 0.000222 \\ -0.002432 & -0.000148 & 0.14452 & 0.005048 & -0.007181 & 0.000141 & -0.671045 & -0.006764 \\ 0.092121 & 0.005593 & 0.002964 & 0.000104 & 0.515088 & -0.010083 & 1.119107 & 0.01128 \\ 0.011063 & 0.000672 & 0.001836 & 0.000064 & 0.063652 & -0.001246 & 0.138433 & 0.001395 \end{pmatrix} \tag{4.16}$$

The time-dependent “load” vector in the general modal transformed equations (3.27) is now calculated to:

$$\begin{bmatrix} g_1(t) \\ h_1(t) \\ \cdots \\ g_4(t) \\ h_4(t) \end{bmatrix}^{L} = \boldsymbol{Y_L}^{-1} \cdot \boldsymbol{A^T}\left[\boldsymbol{p}\right] = \begin{pmatrix} -107.534\ u^2 \\ 1829.22\ u^2 \\ -4.12694\ u^2 \\ 125.051\ u^2 \\ -57.5993\ u^2 \\ -2678.55\ u^2 \\ -30.0795\ u^2 \\ 3691.85\ u^2 \end{pmatrix} \tag{4.17}$$

After step-by-step integration of the four modal equations, the time series of the modal coordinates $x_j(t)$, $y_j(t)$, $(j = 1,...4)$, are obtained - Figures 7 - 8:

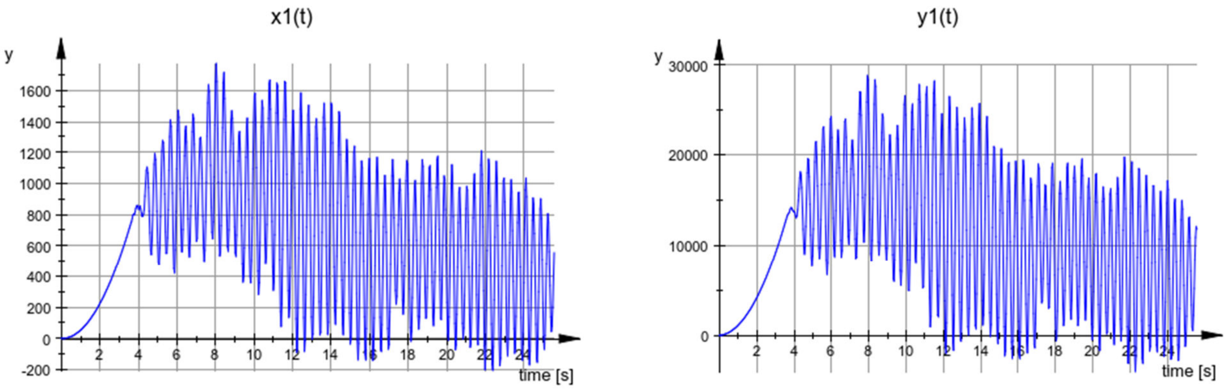

Fig. 7 - Time response of the modal coordinates $\boldsymbol{x_1(t)}, \boldsymbol{1(t)}$ for the case “proportional damping”

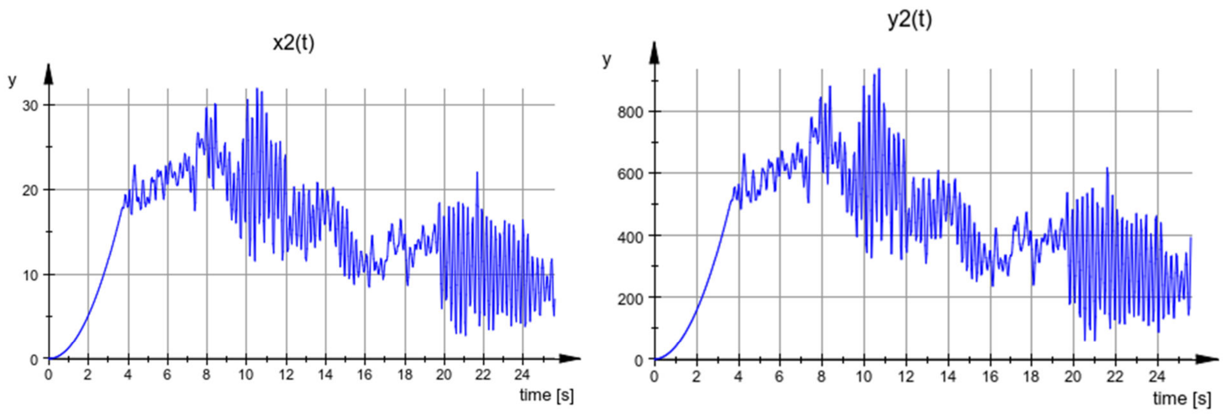

Fig. 8 - Time response of the modal coordinates $\boldsymbol{x_2(t)}, \boldsymbol{y_2(t)}$ for the case “proportional damping”

The total responses $\boldsymbol{V}(t)$, $\dot{\boldsymbol{V}}(t)$ - see Figs. 9-11, are computed by a back transformation according to Eq. (3.30).

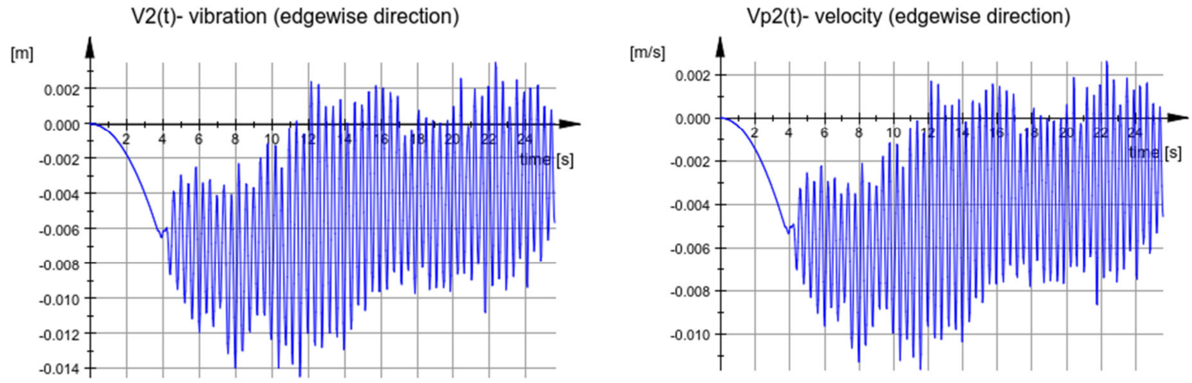

Fig. 9 - Total vibration resp. velocity $u_2(t), \dot{u}_2(t)$ (in y- direction) at the rotor blade tip - node #10

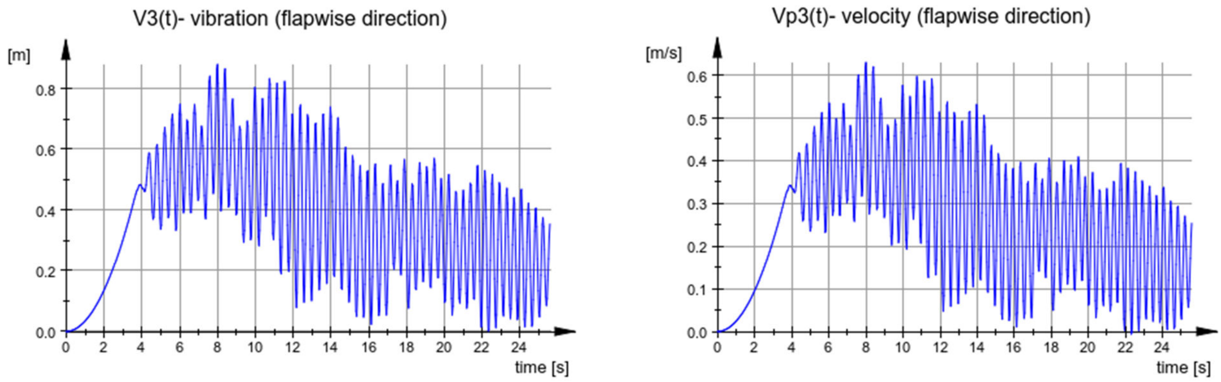

Fig. 10 - Total vibration resp. velocity $u_3(t), \dot{u}_3(t)$ (in z- direction) at the rotor blade tip - node #10

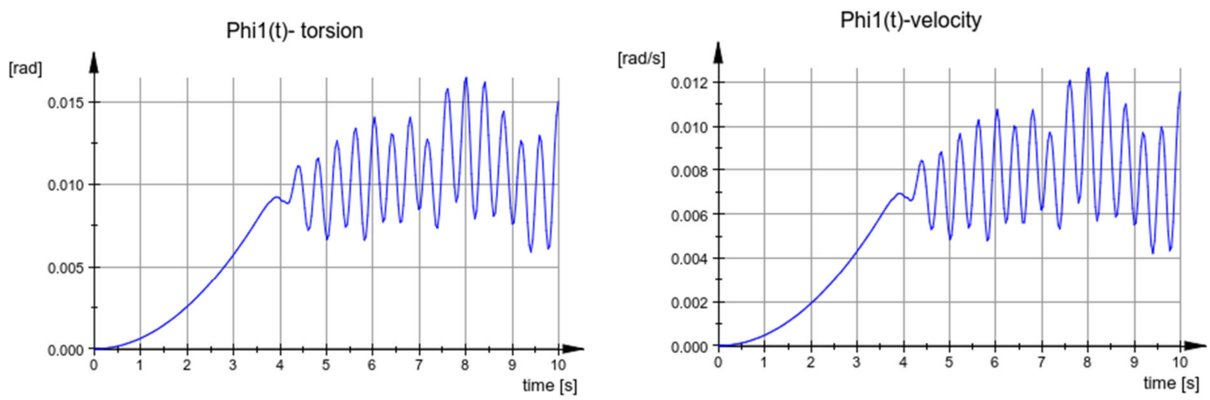

Fig. 11 - Torsional rotation resp. velocity $\varphi_1(t)$, $\dot{\varphi}_1(t)$ at the rotor blade tip - node #10

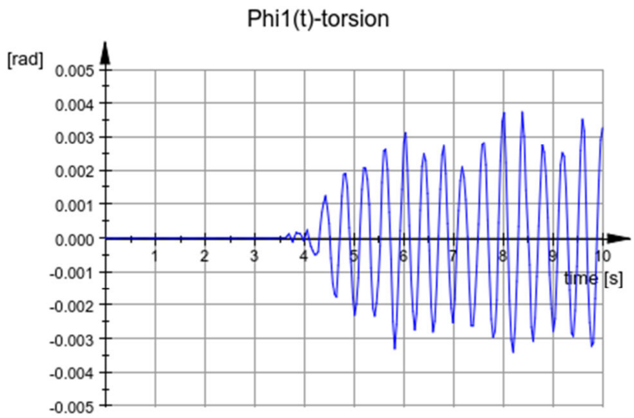

Fig. 12 - Total torsion $\varphi_1(t)$ $[rad]$ at node #10, calculated by direct step-by-step integration ("proportional damping")

The time series for the DOF calculated by direct step-by-step integration of the equations of motion (2.1) are practically identical to the vibrations in Figures 9-11. The only difference occurs in the torsional vibration, compare Figures 11 and 12. The deviations may be explained by the absence of a torsional eigenmode in the four employed eigenmodes in the modal matrix.

5 RESULTS AND CONCLUSIONS

In the first variant (Sec. 2) of the proposed procedure the real transformation matrix is assembled employing the right complex conjugate eigenvector pairs, normalized on the SDOFS level and on MDOFS level with respect to the corresponding mass matrix. There are shown and discussed in details advantages and differences in comparison with a similar method (Fai F. Ma, 2010), (Fai F. Ma, 2011) called "phase synchronization", which is based on the "Lancaster" space state form of the equations of motion. The proposed procedure is derived in a quite natural way, but it doesn't base on the notion of "phase synchronization".

The second presented variant (Sec. 3) operates with both the right and the left complex eigenvector pairs. In this version the eigenvectors for the MDOFS are normalized by using the orthogonality relationships between the right and left complex eigenvectors.

In both proposed procedures the real-space modal transformation matrix $\boldsymbol{Y}$ is developed by combining of two complex transformations, resulting from the eigenvalue problem of the SDOFS and the MDOFS. Analytical expressions for the real-space transformation matrix and for the real-space "right side" vector of the uncoupled modal equations are derived.

Both presented variants of the modal procedure retain the common advantages of the classic modal decomposition of the equations of motion. An uncomplete modal transformation may be performed by use of a few $(k << n)$ eigenmodes to transform the state space equations into k uncoupled SDOFS block equations in real space. Employing only the k lowest eigenvector pairs in the $\boldsymbol{Y}$ -basis is leading with sufficient numerical accuracy to the total time response of all original n DOF - as shown in the numerical example in Sec. 4.

A structural-mechanical example with 54 DOF - vibration of a wind turbine rotor blade subjected to wind thrust loads - demonstrates the performance of the second presented modal procedure (Sec.3) for two cases - non-proportional and proportional (Rayleigh) damping.

REFERENCES

[1] A.K. Chorpa, Dynamics of Structures. Theory and Applications to Earthquake Engineering, Pearson Prentice Hall, New Jersey, 2007.

[2] E. Stanoev, Eine alternative FE-Formulierung der kinetischen Effekte beim räumlich belasteten Stab. Rostocker Berichte aus dem Institut für Bauingenieurwesen, Heft 17, Universität Rostock, Institut für Bauingenieurwesen, 2007, ISSN 1438-7638, pp.143-161.

[3] E. Stanoev, A modified modal analysis method for damped multi-degree-of-freedom-systems in structural mechanics. Zeitschrift für angewandte Mathematik und Mechanik (ZAMM), 2013, 1 - 23 (2013), http://onlinelibrary.wiley.com/doi/10.1002/zamm.201300061/abstract.

[4] E. Stanoev, A modal analysis method for structural models with non-modal damping, MS “Multibody system dynamics and modal reduction” in the frame of 11th World Congress on Computational Mechanics (WCCM XI), 5th European Conference on Computational Mechanics (ECCM V), 20-25 Juli 2014, Barcelona, ISBN: 978-84-942844-7-2, Tomo IV, pp. 3034-3045.

[5] E. Stanoev, A real-space modal analysis method for non-proportional damped structures, MS 918 “Computer algebra systems in modelling static and dynamic problems in mechanics of solids” in the frame of the ECCOMAS Congress 2016 (VII European Congress on Computational Methods in Applied Sciences and Engineering), 5-10 Juni 2016, Crete Island, Greece, https://www.eccomas2016.org/proceedings/ pdf/5682.pdf.

[6] E. Stanoev, Modal analysis procedure using complex left and right eigenvectors of non-proportionally damped structures, RS 12 ”Numerical simulation methods for dynamic problems” in the frame of COMPDYN 2017 (6th ECCOMAS Thematic Conference on Computational Methods in Structural Dynamics and Earthquake Engineering), 15-17 June 2017, Rhodes Island, Greece,https://2017.compdyn.org/proceedings/pdf/17160.pdf.

[7] Fai F. Ma, A. Imam, M. Morzfeld, The decoupling of damped linear systems in oscillatory free vibration, Journal of Sound and Vibration 324 (2009), pp. 408-428.

[8] Fai F. Ma, M. Morzfeld, A. Imam, The decoupling of damped linear systems in free or forced vibration, Journal of Sound and Vibration 329 (2010), pp. 3182-3202.

[9] Fai F. Ma, M. Morzfeld, The decoupling of damped linear systems in configuration and state spaces, Journal of Sound and Vibration 330 (2011), pp. 155-161.

[10] H. Cramer, E. Stanoev, Ein Verfahren zur modalen Analyse gedämpfter Systeme der Strukturmechanik. Rostocker Berichte aus dem Institut für Bauingenieurwesen, Heft 19, Universität Rostock, Institut für Bauingenieurwesen, 2008, ISSN 1438-7638, pp. 83-107.

[11] H. J. Peters, P. Tiso, J.F.L. Goosen, F. van Keulen, Modifying resonance modes of dissipative structures using magnitude and phase information, 11th World Congress on Computational Mechanics (WCCM XI), 5th European Conference on Computational Mechanics (ECCM V), 20-25 Juli 2014, Barcelona, ISBN: 978-84-942844-7-2, Tomo II, pp. 489-500.

[12] K. Meskouris, Baudynamik - Modelle, Methoden, Praxisbeispiele, Ernst & Sohn, 1999.

[13] M. Géradin, D. Rixen, Mechanical vibrations - theory and applications to structural dynamics, John Wiley & Sons Ltd, 1997-

[14] M. T. Chu, N. T. Buono, Total decoupling of general quadratic pencils, Part I: Theory, Journal of Sound and Vibration 309 (2008), pp. 96-111.

[15] M. T. Chu, N. T. Buono, Total decoupling of general quadratic pencils, Part II: Structure preserving isospectral flows, Journal of Sound and Vibration 309 (2008), pp. 112-128.

[16] M.-C. Kim, L.-W. Lee, Eigenproblems for large structures with non-proportional damping. Earthquake Engng. Struct. Dyn, 28, pp. 157-172, 1999.

[17] Nan Li, Berechnung der Querschnittssteifigkeiten des Rotorblatts einer WEA durch ein FE-Verfahren für dünnwandige mehrzellige Profile mit Einsatz von MATLAB, Studienarbeit, University of Rostock, Endowed Chair of Wind Energy Technology, 2015.

[18] P. Lancaster, Lambda-Matrices and Vibrating Systems, Pergamon Press, Oxford, United Kingdom, 1966.

[19] S.D. Garvey, M.I. Friswell, U. Prells, Co-ordinate transformations for second order systems, I: general transformations, Journal of Sound and Vibration 258 (2002), pp. 885-909.

[20] S.D. Garvey, M.I. Friswell, U. Prells, Co-ordinate transformations for second order systems, II: elementary structure-preserving transformations, Journal of Sound and Vibration 258 (2002), pp. 911-930.

[21] T. Burton, N. Jenkins, D. Sharpe, E. Bossanyi, Wind Energy Handbook, John Wiley & Sons, 2011, chapter 5.7, 5.8.

[22] T.K. Caughey, M.E.J. O'Kelly, Classical normal modes in damped linear dynamic systems, ASME Journal of Applied Mechanics 32 (1965), pp. 583-588.

[23] T.K. Caughey, F. Ma, Complex modes and solvability of non-classically damped linear systems, ASME Journal of Applied Mechanics 60 (1993), pp. 26-28.